



NTNU – Trondheim
Norwegian University of
Science and Technology

Energy Considerations of Initiation of Fast Streamers in Cyclohexane

Au-Dung Vuong

Master of Science in Physics and Mathematics

Submission date: June 2015

Supervisor: Arne Mikkelsen, IFY

Co-supervisor: Øystein Hestad, SINTEF Energi

Norwegian University of Science and Technology
Department of Physics

Acknowledgements

I would like to thank my supervisor Øystein Hestad for guidance and support with my master thesis and also for the opportunity to be a part of SINTEF Energy's research project. His colleagues Dag Linhjell, Lars Lundgaard and Torstein Grav and professor Per-Olof Åstrand at the Department of Chemistry at NTNU have also been very helpful during the work with my thesis.

I am forever grateful for the support and encouragement from my family and friends. Huge thanks go to Jon FUSDahl, Kjersti S. Krakhella, Maria K. Eikland Bækkelie and Stine B. Vennemo for helping me so much with my thesis. You have no idea how much I appreciate it.

I also want to thank my supervisor at the Department of Physics at NTNU, Arne Mikkelsen, for making it possible to this work.

Table of Contents

Problem Description	v
Sammendrag	vi
Summary	vii
Notation	viii
1 Introduction	1
2 Theory	3
2.1 The Nature of Streamers	3
2.1.1 Streamers in Gas	3
2.1.2 Streamers in Liquid	4
2.1.3 Initiation of Streamers	7
2.1.4 Propagation of Streamers	7
2.1.5 Stopping of Streamers	8
2.1.6 Factors Affecting the Initiation and Propagation of Streamers	9
2.2 Modeling the Streamer as a Rotational Hyperboloid	11
2.2.1 Available Energy as the Streamer Grows	11
2.3 Heating and Evaporating the Streamer	13
2.3.1 Energy Needed to Heat the Streamer	13
2.3.2 Cyclohexane's Heat Capacity	13
2.3.3 Pressure Relaxation	14
2.4 Decomposition of Cyclohexane	15
2.4.1 Transition State Theory	17
2.4.2 Estimating the Rate Coefficients for the Reverse Reaction	19
2.4.3 Energy Needed to Decompose Cyclohexane	20

3	Method	23
3.1	Calculating the Available Energy	24
3.2	Kinetic Monte Carlo Simulation	24
4	Results	27
4.1	Energy Stored in the Electric Field	27
4.2	Heating the Streamer	27
4.2.1	Regression of Cyclohexane's Heat Capacity	27
4.2.2	Energy Needed to Heat and Evaporate the Streamer	27
4.3	Decomposition of Cyclohexane	30
4.3.1	Estimating Gibbs Free Energy	30
4.3.2	The Ring Opening Process	32
4.3.3	Energy Needed for Decomposition	38
5	Discussion	41
5.1	Heating the Streamer	41
5.1.1	Temperature in the Streamer	41
5.1.2	The Streamer Radius	42
5.1.3	Laplacian Field vs. Space Charge Limited Field	42
5.2	Decomposing Cyclohexane	43
5.2.1	The Decomposition Products	43
5.2.2	The Energy Needed to Decompose Cyclohexane	44
5.3	Ionizing the Gas	44
6	Conclusion	45
	Bibliography	47
	Appendix	I
A	MATLAB code	I
A.1	diff_energy.m	I
A.2	plot_energy.m	II
A.3	Temp.m	II
B	Python code	V
B.1	Cyclohexane.py	V

Problem Description

The energy in the initiation of a fast streamer in cyclohexane is considered. When enough voltage is applied to a needle-plan gap, a fast streamer is initiated. The available energy when the streamer initiates is estimated. This thesis will discuss how much of the available energy will heat, vaporize, decompose and ionize the liquid in the streamer, in order to determine some properties of the initiated streamer.

Sammendrag

Hensikten med masteroppgaven er å forbedre en modell av initiering og propagering av "streamere" i dielektrisk væske av Hestad et al. ved Sintef Energi, ved å betrakte energien i en andreordens streamer. Dette er viktig ettersom mer innsikt om prosessene som forårsaker utladninger i væske, kan øke den forventede levetiden til isolasjonsvæsker.

I modellen ble en nål-plankonfigurasjon brukt, hvor elektrodespissen ble representert av en rotasjonshyperboloide og den dielektriske væsken var sykloheksan. Når en spenning ble påtrykt, ble en tynn kanal ionisert og gjort ledende av det sterke elektriske feltet. Energien etter det elektriske feltet endret seg, ble beregnet i "finite element"-analyseprogramvaren Comsol. Det ble antatt at den tilgjengelige energien gikk med til oppvarming, fordamping, oppbryting og ionisering av sykloheksan. Kinetisk Monte Carlo-simulering ble gjort for å forutsi hva sykloheksan brytes opp til.

Den initielle streameren hadde radius $c_r = 0,1 \mu\text{m}$ og lengden $c_l = 8 \mu\text{m}$. Den besto av gass med en temperatur på $T = 1485 \text{ K}$, der gassen var delvis ionisert. På grunn av temperaturstigningen, utvidet radien seg til $c_{r-exp} = 24 \mu\text{m}$. Temperaturen i streameren var for lav til å bryte opp sykloheksan, men på en annen side var energien som trengs for å bryte opp syklohexan når $T = 3000 \text{ K}$ bare 1% av fordampingsenergien. Dermed ville oppbrytning mest sannsynlig ha skjedd hvis temperaturen i streameren var høy nok. Sammenlignet med observasjoner for andre ordens streamere, var temperaturen i modellen for lav og radien var for stor.

Summary

The purpose of this thesis is to improve a model of streamer propagation in dielectric liquid by Hestad et al. at Sintef Energy Research, by considering the energy in an initiated second mode streamer. This is important, as more knowledge of the processes that cause discharges in liquid, may increase the lifetime expectancy of insulator liquids.

In the model a needle-gap configuration was used, where the electrode tip was modeled as a rotational hyperboloid and the dielectric liquid was cyclohexane. When a voltage was applied, a thin channel was ionized and made conducting by a strong electric field. The energy difference after the electric field redistributes, was calculated in the finite element analysis software Comsol. It was assumed that the available energy would heat, evaporate, decompose and ionize cyclohexane. Kinetic Monte Carlo simulation was done to predict what cyclohexane decomposes to at high temperatures.

The initial streamer had the radius $c_r = 0.1 \mu\text{m}$ and the length $c_l = 8 \mu\text{m}$. It consisted gas with the temperature $T = 1485 \text{ K}$, where parts of it were ionized. Due to the temperature rise, the radius expanded to $c_{r-exp} = 24 \mu\text{m}$. The temperature in the streamer was too low to decompose cyclohexane. However, the energy needed to decompose cyclohexane at $T = 3000 \text{ K}$ was only 1% of the vaporization energy. Therefore the decomposition would most likely have happened if the temperature in the streamer had been high enough. Compared to observations of second mode streamers, the temperature was too low and the radius was too big.

Notation

Relevant Concepts

- Anode - positive polarity electrode.
- Breakdown voltage - the voltage that has 50% probability of causing breakdown.
- Cathode - negative polarity electrode.
- Electron avalanche - a chain reaction where an electron, subjected to an electric field, collides with other atoms and ionizes them by impact ionization. The new electrons will keep ionizing other atoms.
- Field emission current - a current injected from an electrode to a liquid due to the strong electric field.
- Impact ionization - ionization caused by a collision between molecules.
- Initiation voltage - the voltage that has 50% probability of initiating a slow streamers
- Partial discharge - localised electric breakdown of a part of a liquid, which is not bridged between the conductors.
- Propagation voltage - the voltage that has 50% probability of initiating second mode streamers
- Thermal ionization - ionization due to a high temperature.

Symbols

List of the most important physical quantities used in this thesis with their units.

- C_p - heat capacity [J/(Kmol)]
- c - concentration [1]
- c_l - streamer length [μm]
- c_r - streamer radius [μm]
- D - bond dissociation energy [kJ/mol]

-
- d - gap length [μm]
 - \vec{E} - electric field [V/m]
 - E_a - activation energy [J]
 - G - gibbs free energy [kJ/mol]
 - H - enthalpy [kJ/mol]
 - k - rate coefficient. The unit depends on the reaction.
 - m_M - molar mass [kg/mol]
 - p - pressure [Pa]
 - r - reaction rate [$1/\text{s}$]
 - r_p - tip radius [μm]
 - S - entropy [kJ/mol]
 - T - temperature [K]
 - t - time [s]
 - U - energy [J]
 - U_b - average bond energy [kJ/mol]
 - V - potential [V]
 - v - volume [m^3]
 - ϵ - permittivity [F/m]
 - ρ - density [kg/m^3]

Introduction

Dielectric liquids are typically used as electric insulators in high voltage applications and in subsea equipment. There are several reasons for this. First of all, the dielectric strength, thus the breakdown strength, is higher for liquids than for gases. Solids have even higher breakdown strength than liquids, but liquids are more favorable as insulators, in some cases, as their abilities to recover after a partial discharge are better than the solids'. Second of all, liquids have more efficient cooling effects than solids and gases. These allow equipment with liquid insulator to operate at a lower temperature than equipment with solid or gaseous insulator. As a result the applications will be subjected to less thermal stress and therefore last longer without extra maintenance. Lastly, the high breakdown strength and the high heat capacity cause liquid insulators to be more space efficient than the alternatives [1].

An ideal insulator liquid is refined and is composed of molecules that are electrically neutral and non-polar. The purer the liquid is, the smaller is the chance of having partial discharges in the liquid. Typical insulator liquids are mineral oils, esters and silicone fluids [2]. Unsurprisingly, it is difficult to achieve ideal insulators in reality. The insulator liquids will always contain some sort of impurities that will enhance partial discharges. Discharges that create a conducting area with another refractive index than the surrounding area's, are called streamers. The streamers are often filamentary and can be observed with shadowgraphic methods. A streamer that is bridged between two conductors can cause a breakdown. Even though the liquid insulator is self-healing, frequent discharges will gradually weaken the insulator and the equipment may get serious damages. Since the lifetime for electrical equipment often is limited by the lifetime of the insulator, it is advantageous to understand the physics behind streamers to be able to increase the lifetime expectancy of insulator liquids, and thus also electric applications.

The study of streamers has been going on for a few decades. When study-

ing streamers, a needle-plane geometry is often used. The electric field from this geometry resembles the field from sharp-edged impurities that are attached to conductors. In addition relatively low voltages can generate high electric fields in this configuration. In 1981, Devins, Rząd and Schwabe did a comprehensive study of both positive and negative streamers in a needle-plane gap [3]. Lesaint and Masala characterized the different propagation modes in 1998 [4] and lately, SINTEF Energy Research and ABB have been working on simulating the propagation of streamers in dielectric liquids. In [5], a simple numerical calculation is done based on the Townsend-Meek criterion, where electrons are randomly distributed in the liquid. At lower voltages the simulation shows a similar trend to the experimental results, but in the model, the branching of streamers is not well defined and the transitions between propagation modes are somewhat unclear. To make the model more accurate, the energy in the process must be considered.

In this thesis characteristics of streamers in liquid will be presented, theories for the initiation and propagation of streamers are discussed, and how streamers are classified and what factors affect their propagation will be described. The energy released when the streamer is formed will be calculated. Lastly, the available energy distribution will be considered and discussed. The motivation for this work is to make further improvements of the model by Hestad et al. [5].

Theory

2.1 The Nature of Streamers

2.1.1 Streamers in Gas

In gas theory the streamer mechanism is a well-known phenomenon [1]. This is why streamer initiation and propagation in liquid are often explained by using the streamer mechanism in gas.

An inhomogeneous electric field is set up by applying a voltage over a needle-plane gap. The polarity of the needle can be either positive or negative, but for now it is assumed to be positive. Between the gap, there will be a few seed electrons due to electron injection from the cathode, field ionization and/or thermal ionization. These electrons will move towards the anode, where the electric field is strongest. As the electrons are moving, they will collide with other gas molecules and may ionize them. The newly detached electrons will then start to move towards the anode, while heavier positive ions are left behind, creating a local positive electric field. As this process repeats itself, a channel of ions is created and hence the so-called streamer propagates. A positive streamer refers to a system with a point anode and a negative streamer refers to a system with point cathode. Figure 2.1 illustrates how positive streamers are initiated and propagate through a gas.

The streamer mechanism depends on electron collisions and seed electrons, which are stochastic events. Consequently an applied voltage may be the initiation voltage for one certain event, but not for all.

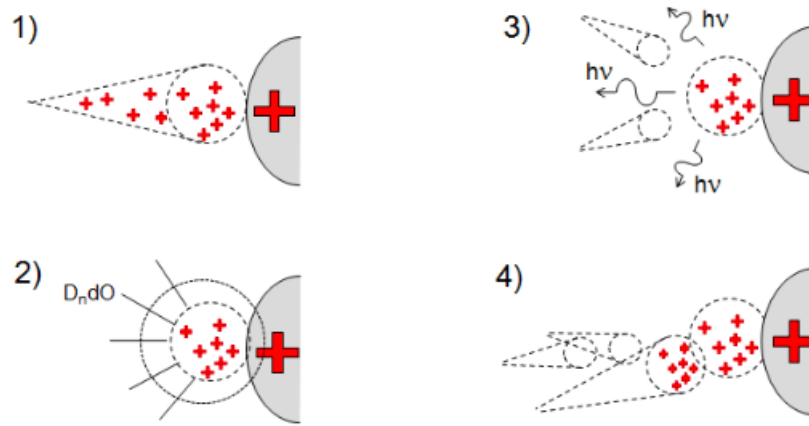


Figure 2.1: Initiation and propagation of a positive streamer in gas. A strong electric field induces electrons by field ionization or/and impact ionization. 1) The free electrons move through the gas and towards the anode. 2) The heavier positive ions are left behind and set up a "new" positive electric field close to the anode. 3) The electric field from the "extended electrode tip" causes field ionization and impact ionization. 4) A chain reaction is started and a channel of charge carriers, also known as the streamer, will expand. [1].

2.1.2 Streamers in Liquid

It is a common perception among scientists that the electrons' mean free path in liquid is too short for impact ionization to occur. Therefore the streamer mechanism in gas cannot be directly applied to liquids. If the electric field is strong enough, it is assumed that electron avalanches can initiate in the liquid, but for weaker fields another theory is more likely to apply [6]. Figure 2.2 and 2.3 shows experimentally observed positive and negative streamers in cyclohexane.

The higher voltage applied, the more current will propagate in the streamer. As a result of this, the streamer glows more. The streamer's projection can then be identified by shadowgraphic images and oscilloscope recordings. Based on the streamer velocity, the streamer can be classified as different propagation modes. There are four different modes for positive streamers and three different modes for negative streamers [8]. The first positive and negative modes are classified as slow streamers and propagate at velocities in the order of 100 m/s. The slow streamers appear at low voltages and have a bush-like shape with channels consisting of gas bubbles [4].

As the applied voltage increases, the propagation velocity increases and the streamer travels farther as well. Second mode streamers are initiated when the applied voltage, is above the propagation voltage V_p . They propagate with velocities up to a few km/s and are more filamentary and less branched than the first

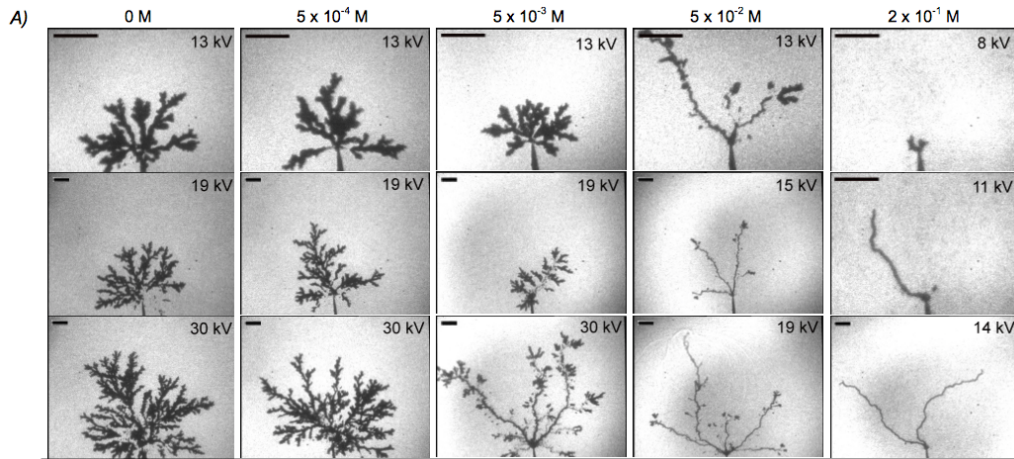


Figure 2.2: Shadowgraphic images of positive streamers in cyclohexane with different concentrations of tetramethyl-p-phenylenediamine and at different applied voltages [7].

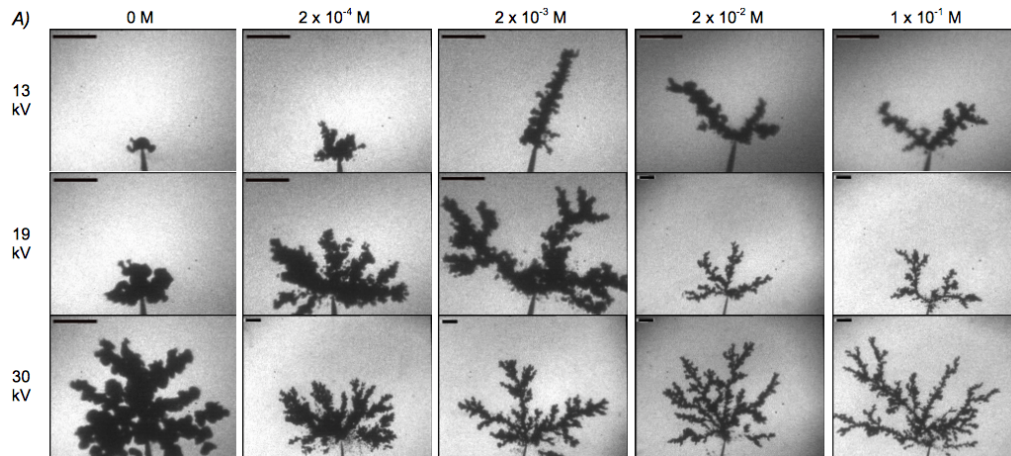


Figure 2.3: Shadowgraphic images of fully developed negative streamers in cyclohexane with different concentrations of perfluoromethylcyclohexane and at different applied voltages [7].

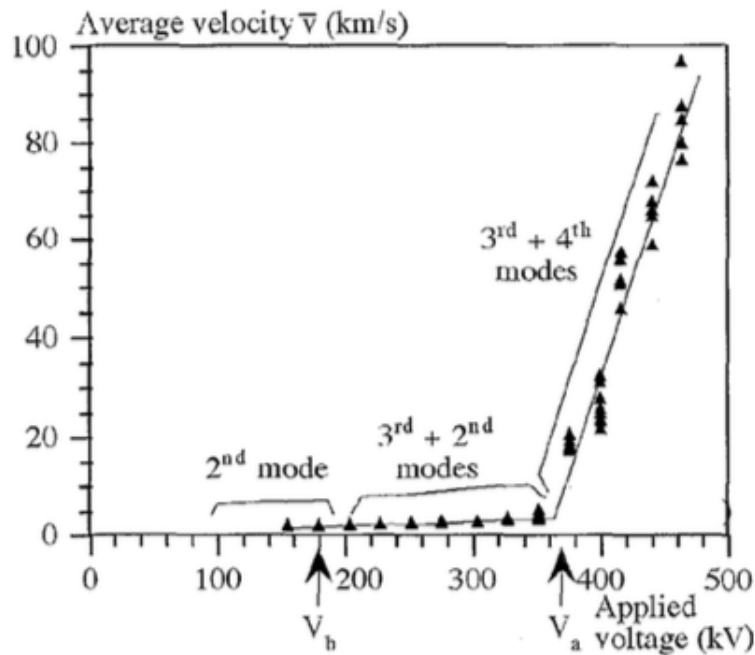


Figure 2.4: Average propagation velocity as a function of applied voltage. V_b is the breakdown voltage and V_a is the acceleration voltage; the threshold for when the propagation velocity depend strongly on applied voltage [4].

mode streamers [9][4]. Second mode streamers are considered as fast streamers. As the energy is higher in these streamers, the streamer temperature is higher as well. Consequently the degree of ionization is higher which leads to a higher conductivity. An increasing temperature may also decompose the liquid [10].

Third mode streamers are similar to second modes, but they propagate with velocities from 10 to 20 km/s. Streamers with velocities greater than 100 km/s are classified as fourth modes [9]. As these streamers are very fast and breakdown occurs quickly, it is difficult to get detailed information about fourth mode streamers. The faster the streamer is, the more filaments it has. Unlike the two slower modes, the propagation velocity for third and fourth modes depends strongly on applied voltage [9]. Figure 2.4 shows how the propagation velocities for positive streamers depend on applied voltage. Higher propagation voltage means that the streamer propagates farther. Positive streamers travel generally faster than negative streamers for higher voltages, which is why the breakdown voltage is lower for positive streamers than for negative streamers [11].

2.1.3 Initiation of Streamers

Figures 2.2 and 2.3 show that negative streamers are generally bushier than positive streamers, which are more filamentary. In addition the initiation voltage for negative streamers is generally lower than for positive streamers. It is therefore reasonable to believe that the initiation of positive streamers is different from the initiation of negative streamers.

The initiation of negative streamers is pressure-independent for pressures up to 12 MPa [12]. For slow streamers a negative needle-plane electrode will ionize the liquid in front of the electrode tip. The induced electrons will collide with the molecules in the liquid and evaporate them so quickly that shock waves are emitted. In the wake of these, micro bubbles will develop. Due to the phase change, the pressure in the gas bubbles is increased and the bubbles will expand in a few microseconds. After they have reached a critical volume and the density is low enough, the electron's mean free path is long enough for the occurrence of partial discharges in the gas [10].

Several explanations for how positive streamers initiate have been proposed, but none of them are compatible with all the experimental observations. It is suggested that the initiation of positive streamers happens in gas-phase as the initiation voltage increases when the hydrostatic pressure increases [12]. Jones and Kunhardt propose a theory where the area closest to the electrode tip is heated due to field emission currents from the electrodes [6]. If there is enough energy, the heating will lead to evaporation of the liquid, which will decrease the density in the area around the electrode tip. A lower density increases the electrons mean free path. As a result electron avalanches can occur, and this may lead to streamer initiation. Lewis has another theory where, in short time scales, the dielectric liquid has solid-like properties and the electric field will excite electrons and generate holes. This leads to a lower density area, which will enhance the growth of streamers [13].

Jones and Kunhardt mention that the propagation velocity in the bubble formation is too slow compared to the fastest observed streamers. The bubble theory is then not sufficient to explain the propagation of fast streamers. This is why it is believed that the strong electric field will ionize the liquid and enhance electron avalanches in it [3][6].

2.1.4 Propagation of Streamers

Slow streamers propagate as repetitive discharges occur in the gas bubbles [8]. As already mentioned, impact ionization occur in the gas when the density is low enough. For positive streamers the generated electrons will travel towards the anode and leave the positive ions in the gas. The low-density area serves as

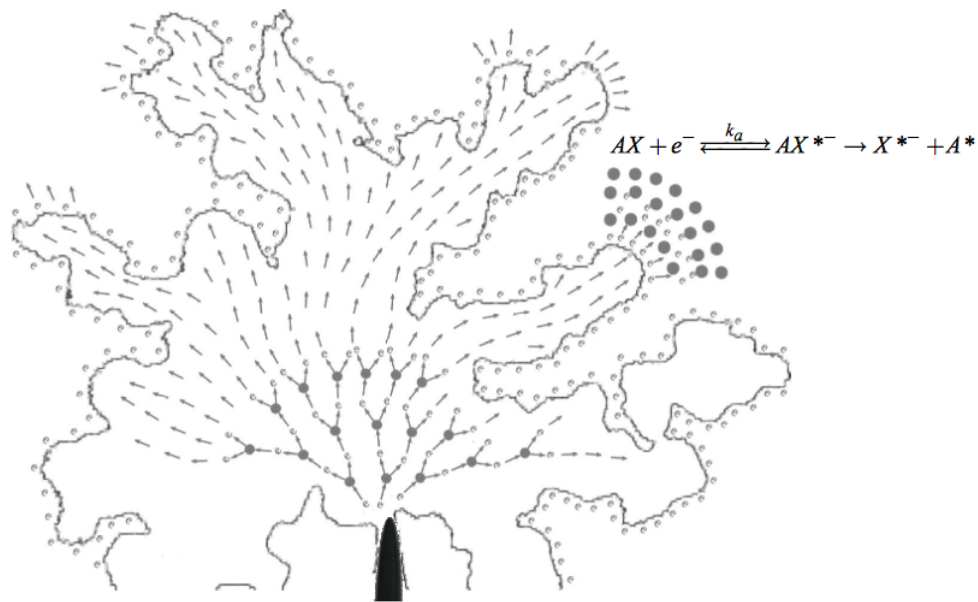


Figure 2.5: Propagation of slow negative streamers in liquid. Partial discharges occur in the low-density area at the tip of the cathode. The induced electrons move towards the anode and collide with the liquid in front of the gas. The liquid is heated, maybe evaporated and the chain reaction goes on until the electric field is too weak [8].

a positively charged streamer tip that will heat the liquid around it and extend the "streamer tip". For negative streamers the electrons in the gaseous area will move towards the anode and collide with liquid in the gas-liquid interface. The collision heats and evaporates the liquid and creates a new low-density area. A chain reaction is started and the streamer "propagates". Figure 2.5 illustrates the propagation of a slow negative streamer.

Fast streamers in liquid propagate in the same way as streamers in gas. Free electrons in the liquid, caused by impact ionization or field ionization, move towards the positive electrode. On their way, they collide with molecules that may start an electron avalanche. As the avalanches move towards the anode, positive ions are left behind and create an extended positive streamer tip. As the ionized region grows, the streamer "propagates". The propagation of fast streamers in liquid is illustrated in Figure 2.6.

2.1.5 Stopping of Streamers

The electric field in a needle-plane configuration diverges rapidly as the distance from the needle increases. The streamer will propagate until the electric field at the streamer tip is too weak for ionization to occur. When the energy is insuffi-

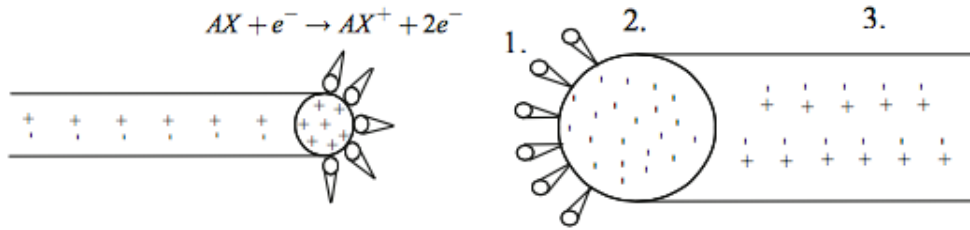


Figure 2.6: Propagation of fast positive and negative streamer in liquid. Electrons, caused by impact ionization or direct field ionization, move towards the positive electrode. The heavier positive ions left behind and connect the streamer to the needle electrode. The streamer expands as the electric field at the streamer tip keeps ionizing the liquid in front of it [8].

cient, the streamer stops growing and eventually it quenches [14]. If the hydrostatic pressure is too high, the streamer stops growing due to collapsing of the gas filaments rather than due to the divergent electric field [15].

2.1.6 Factors Affecting the Initiation and Propagation of Streamers

Geometry Effects

The smaller the tip radius is, the stronger the electric field. This means that less applied voltage is needed to initiate streamers. The initiation voltage will therefore increase when the tip radius increases, which is illustrated in Figure 2.7. [16].

When it comes to the electrode gap distance, the electric field strength increases as the gap distance decreases. Thus for smaller gap distances, the initiation voltage decreases and the propagation velocity increases [17][3]. For positive polarity the propagation velocity is constant over the gap. This is not the case for negative streamers [3]. In addition to the electrode's geometry, the initiation voltage also depends on the shape of the applied voltage pulse. A pulse with a longer rise time will increase the initiation voltage. As the voltage rises, space charges will build up around the electrode tip. Longer rise time allow more space charges to build up, which creates a stronger screening effect. Accordingly a higher voltage is needed to initiate a streamer [17].

Pressure Effects

Devins et al. varied the hydrostatic pressure from 0 to 1 atm in their experiments with Marcol 70 [3]. When the applied voltage was 40 kV, the streamer's propa-

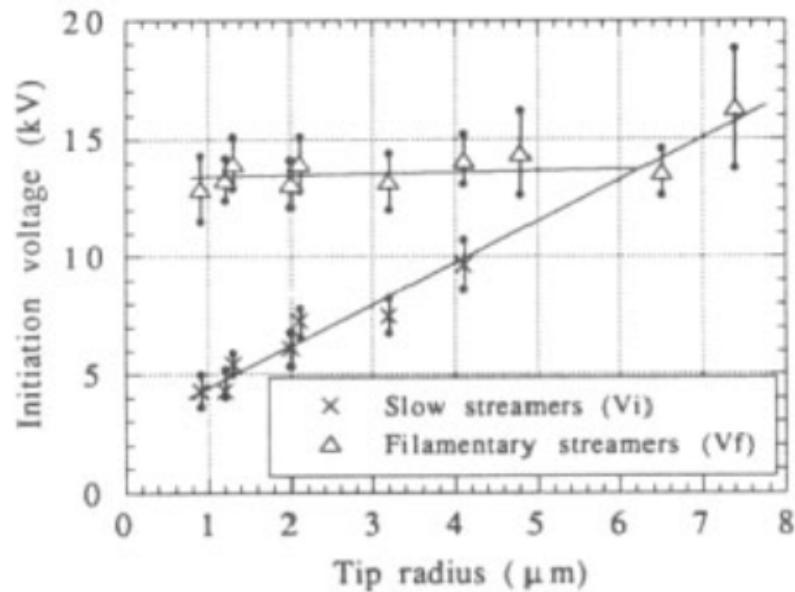


Figure 2.7: How initiation and propagation voltage depends on the electrode tip radius in cyclohexane [16]. The gap spacing is $d = 2.5$ mm and the rise time of the voltage is $t_r = 15$ ns. Slow "bush-like" streamers are initiated when the voltage $V > 4$ kV and the tip radius $r > 0.8$ μm . When $V > 14.5$ kV the streamers are fast.

gation velocity increased for decreasing pressure, but showed no dependence of the pressure when the applied voltage was 90 kV. Lesaint and Gournay did the same experiment for cyclohexane and pentane for pressures between 0 and 8 MPa [18]. The results show that changing the pressure does not affect the propagation velocity, but rather the length and diameter of the streamer. When the hydrostatic pressure is high, more energy is needed to heat and evaporate the streamer to prevent the liquid-gas interface from collapsing. Hence increasing the pressure decreases both the stopping length and diameter.

Effects of Additives

According to Ingebrigtsen there are no general correlations between the characteristics of streamer propagation and the liquid's bulk properties, but the propagation velocities are affected by adding molecules with certain properties [8]. Experiments show that electron-attaching additives speed up the propagation velocity for negative streamers while additives with low ionization potential have the same effect on positive streamers [6][7]. In both cases, the structure of the streamer is thinner for higher concentration of additives. Figure 2.2 and 2.3 show how tetramethyl-p-phenylenediamine and perfluoromethylcyclohexane affect positive

and negative streamers respectively.

2.2 Modeling the Streamer as a Rotational Hyperboloid

When doing calculations with streamers, it is useful to model the electrode tip as a rotational hyperboloid. Laplace' equation is then separable and can be solved in prolate spheroid coordinates [19]. The potential is

$$V(\theta) = C \ln \tan \frac{\theta}{2}, \quad (2.1)$$

and the electric field is

$$E = \frac{1}{a\sqrt{\sinh^2 \eta + \sin^2 \theta}} \frac{C}{\sin \theta} \hat{\theta}, \quad (2.2)$$

where η and θ are the prolate spheroid coordinates illustrated in Figure 2.8. The distance from the origin to the hyperbola's focal point is $a \approx d + r_p/2$, where d is the shortest distance from the origin to the hyperboloid and r_p is the approximated point tip radius of the hyperboloid. The constant C is given by

$$C = \frac{V_0}{\ln \tan \left\{ \frac{\pi}{2} - \sqrt{\frac{1-d/a}{2}} \right\}}, \quad (2.3)$$

where V_0 is the applied voltage. At the tip of the electrode, the electric field is [20]

$$E_{tip} = \frac{2V_0}{r_p \ln\left(\frac{4d}{r_p}\right)}. \quad (2.4)$$

2.2.1 Available Energy as the Streamer Grows

The energy required for streamer initiation and propagation is mainly stored in the electric field from the electrodes. Assuming the initiated streamer is of second mode or higher, a channel of liquid will be ionized when a voltage is applied. The initiated streamer channel starts to conduct, the electric field changes and the static energy is released; the energy in the electric field will decrease while the energy in the streamer will increase [3]. When a streamer is initiated, the energy difference due to the redistribution of the electric field is

$$U_{available} = \frac{\epsilon}{2} \int_v \left| \vec{E} \right|^2 dv, \quad (2.5)$$

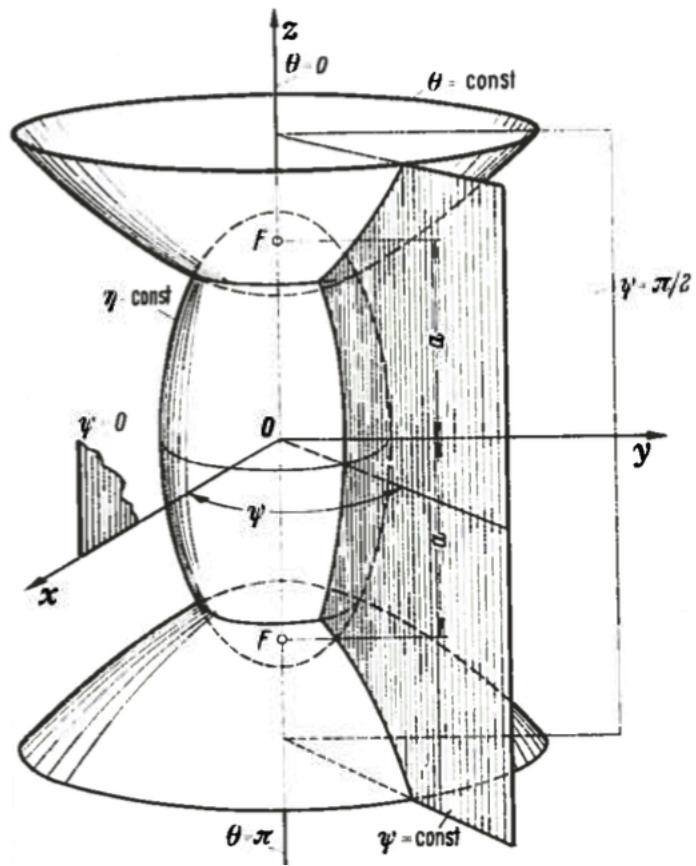


Figure 2.8: Constant curves of η , ξ and θ in prolate spheroid coordinates [19].

where ϵ is the liquid's permittivity and v is the volume of the initiated streamer channel. It is assumed that the dielectric liquid is cyclohexane. Felici discusses how the available energy is distributed as the streamer propagates: In fast streamers, the processes that need most energy are vaporization, decomposition, ionization and displacement [10]. In this thesis the energies for vaporization, decomposition and ionization are considered.

2.3 Heating and Evaporating the Streamer

2.3.1 Energy Needed to Heat the Streamer

When a streamer is initiated, most of the available energy dU will heat and evaporate the liquid. The liquid will first be heated from room temperature T_0 to its boiling point T_b . The energy needed in this process is

$$U_{heating} = \frac{\rho v}{m_M} \int_{T_0}^{T_b} C_p(T) dT, \quad (2.6)$$

where v is the volume of the initiated streamer tip and ρ is the mass density, m_M is the molar mass and $C_p(T)$ is cyclohexane's heat capacity. Assuming the initiated streamer has the geometry in Figure 2.9, the volume of the initiated streamer is

$$v = \pi c_r^2 (c_l - c_r) + \frac{2\pi c_r^3}{3}. \quad (2.7)$$

After the streamer's boiling point is reached, the liquid will evaporate. The energy required in this process is

$$U_{evaporation} = \frac{\Delta_{vap} H \rho v}{m_M}. \quad (2.8)$$

$\Delta_{vap} H$ is the heat of evaporation which is assumed to be independent of temperature. The rest of the energy will increase the gas' temperature from T_b to T_{end} according to equation (2.6).

2.3.2 Cyclohexane's Heat Capacity

A subject's heat capacity is defined as the energy needed to increase its temperature by 1 K. Thus the heat capacity is a measure of the subject's vibrational energy, which depends on the molecule's degrees of freedom. For a general gas molecule with M atoms, where $M > 2$, the degrees of freedom are linearly dependent of M . This is not a rule that applies to all molecules at all temperatures; at low temperatures the vibrational modes are "frozen" and do not contribute to the heat capacity.

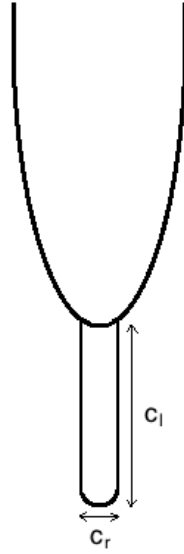


Figure 2.9: The initiated streamer channel is modeled as a cylinder with a hemisphere at the end, where the radius of the cylinder is c_r and the length of the cylinder+hemisphere is c_l .

As the degrees of freedom are closely linked to a molecule's activation energy, Arrhenius' empirical law may be a useful approximation for the heat capacity

$$C_p = C \exp\left(-\frac{E_a}{RT}\right), \quad (2.9)$$

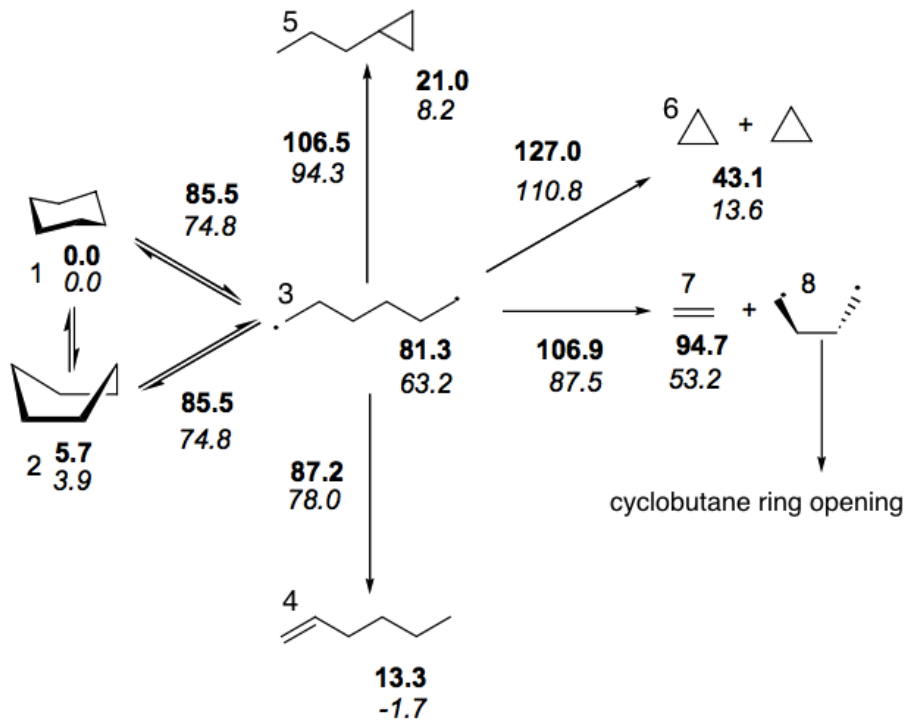
where C is a scaling constant, E_a is the activation energy, R is the gas constant and T is the system's temperature [21].

2.3.3 Pressure Relaxation

Right after initiation of a gaseous streamer channel with volume v_0 , the temperature increases from T_0 to T_{end} . Due to the temperature rise, the hydrostatic pressure in the channel increases. During a few microseconds the channel will expand and the pressure will drop to the surrounding liquid's pressure. It is assumed that the streamer expands adiabatically and that the temperature stays constant in the expansion. By using the ideal gas law, the volume of the streamer channel after the pressure relaxation is

$$v_{end} = v \frac{T_{end}}{T_0}. \quad (2.10)$$

The radius of the expanded streamer can be found by using equation (2.7).

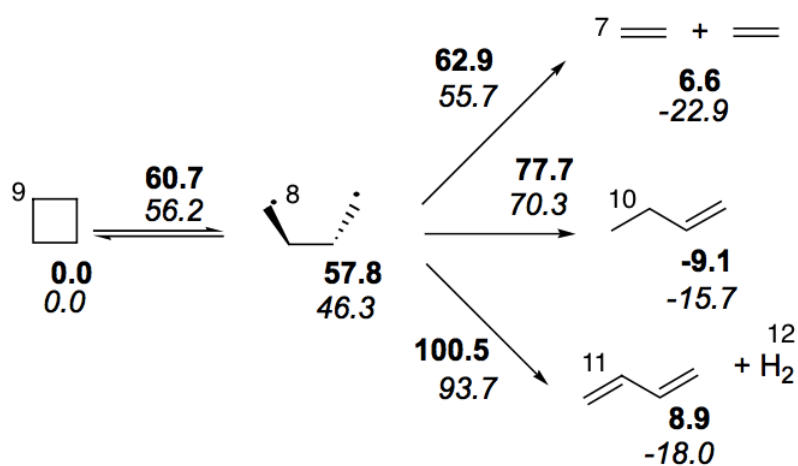


$\Delta G^\circ(T)$ in kcal.mol^{-1} (bold : $T=298\text{K}$, italic : $T=1000\text{K}$)

Figure 2.10: The ring opening process for cyclohexane [24]

2.4 Decomposition of Cyclohexane

In a fast streamer the temperature can reach 2000-7000 K [22]. For relatively high temperatures, molecules will decompose spontaneously. In order to predict how much energy is needed when fast streamers grow, thermal decomposition of cyclohexane is considered. There are two possible initial steps of cyclohexane decomposition; C-H bond scission and C-C bond scission [23]. The first step results in cyclohexyl, while the second step results in biradical 1,6-hexane. As C-C bond scission is more likely to happen than C-H bond scission, only the ring opening will be considered as the initial process. The work presented is based on [24], where transition state theory is used to calculate the rate coefficients for the ring opening of cyclohexane. The most relevant steps in the ring opening process are illustrated in Figures 2.10 and 2.11. The names of the different alkanes are listed in Table 2.1.



$\Delta G^\circ(T)$ in kcal.mol^{-1} (bold : $T=298\text{K}$, italic : $T=1000\text{K}$)

Figure 2.11: The ring opening process for cyclobutane [24]

Table 2.1: The names of the alkanes in Figures 2.10 and 2.11

Molecule number	Molecule name
1	Cyclohexane; chair formation
2	Cyclohexane; boat formation
3	Biradical 1,6-hexane
4	1-hexene
5	Propylcyclopropane
6	Cyclopropane
7	Ethylene
8	Biradical 1,4-butane
9	Cyclobutane
10	1-butene
11	1,3-butadiene
12	Hydrogen

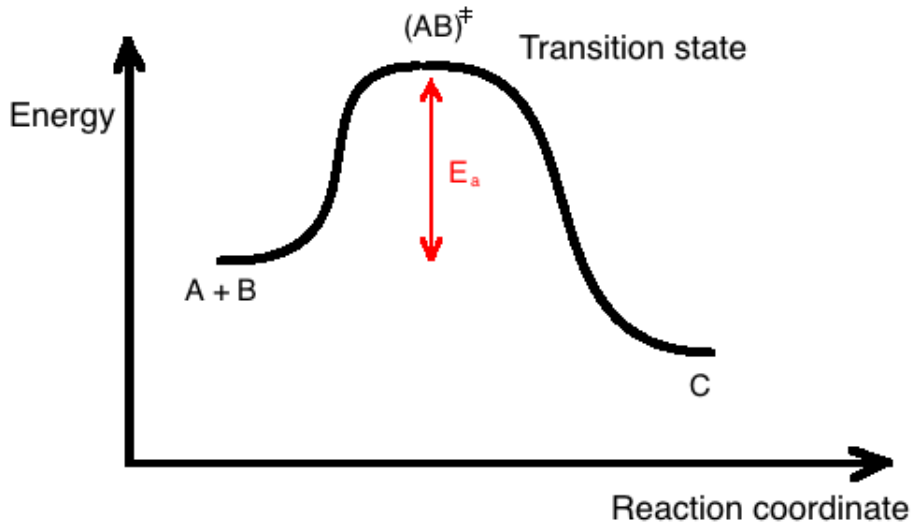


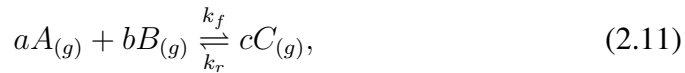
Figure 2.12: A simple process to illustrate transition state theory. The reaction $A + B \rightarrow C$ can be written as $A + B \rightarrow (AB)^\ddagger \rightarrow C$, where $(AB)^\ddagger$ is an unstable transition state.

2.4.1 Transition State Theory

In transition state theory a chemical reaction is divided into two stages. The first stage is a temporary equilibrium between the reactants and an unstable transition state. The second stage is a reaction between the transition state and the products. This is done to better understand how chemical reactions take place. Figure 2.12 illustrates an arbitrary reaction used to easily explain transition state theory.

Calculating the Rate Coefficients

Consider the simple reaction between the two states A , B and C



where k_f and k_r are the forward and reverse rate coefficients, respectively and a , b and c are the stoichiometric coefficients. The variable k_f gives the probability that a molecule of A will convert to molecule B per unit time, while k_r describes the probability for the reverse reaction. If the brackets "[]" indicate the number of molecules or concentration of a molecule, and A , B and C are time dependent, then the rate of change of C is

$$\frac{d[C]}{dt} = k_f[A]^a[B]^b - k_r[C]^c. \quad (2.12)$$

When the reaction has reached equilibrium

$$\frac{d[C]}{dt} = 0 \Leftrightarrow k_f[A]^a[B]^b = k_r[C]^c \quad (2.13)$$

which gives

$$K \equiv \frac{k_f}{k_r} = \frac{[C]_{eq}^c}{[A]_{eq}^a[B]_{eq}^b}, \quad (2.14)$$

where K is the equilibrium constant for equation (2.11).

Calculating the Rate Coefficients by Using Transition State Theory

In transition state theory equation (2.11) is divided into two stages;



where A and B are the reactants, C is the product and $(AB)^\ddagger$ is the temporary, unstable transition state. For simplicity's sake, it is assumed that the stoichiometric coefficients are 1 and that the initial concentration of C is 0. K^\ddagger is the equilibrium constant for the first stage;

$$K^\ddagger = \frac{[(AB)^\ddagger]}{[A][B]}, \quad (2.16)$$

and k^\ddagger is the rate coefficient for the second stage:

$$\frac{d[C]}{dt} = k^\ddagger[(AB)^\ddagger] \stackrel{eq.(2.16)}{=} k^\ddagger K^\ddagger[A][B]. \quad (2.17)$$

This equals equation (2.12), which gives

$$k_f = k^\ddagger K^\ddagger. \quad (2.18)$$

Dill and Bromberg rewrote this to

$$k_f = \frac{k_B T}{h} \overline{K^\ddagger}, \quad (2.19)$$

where k_B is Boltzmann's constant, T is the temperature of the system and h is Planck's constant [21]. $\overline{K^\ddagger}$ has a simple relation to the thermodynamic quantities Gibbs free energy ΔG , enthalpy ΔH and entropy ΔS

$$-k_B T \ln \overline{K^\ddagger} = \Delta G^\ddagger = \Delta H^\ddagger - T \Delta S^\ddagger. \quad (2.20)$$

Substituting equation (2.20) into equation (2.19) gives

$$\begin{aligned} k_f &= \frac{k_B T}{h} \exp\left(-\frac{\Delta H^\ddagger}{k_B T}\right) \exp\left(\frac{\Delta S^\ddagger}{k_B}\right) \\ &= AT \exp\left(-\frac{\Delta H^\ddagger}{k_B T}\right), \end{aligned} \quad (2.21)$$

where ΔH^\ddagger is the same as the activation energy E_a . This equation is known as Arrhenius' empiric equation.

A modified version of this equation is used in [24] to estimate the temperature dependence of the rate coefficients

$$k = AT^n \exp\left(-\frac{E_a}{RT}\right). \quad (2.22)$$

In this equation R is the gas constant, A is the pre-factor and n is a constant. The rate coefficients for the reactions in the ring opening of cyclohexane are listed in Table 2.2. The forward and reverse rate coefficients for the reaction chair-cyclohexane \rightarrow boat-cyclohexane, k_{1-2} and k_{2-1} , can be calculated as

$$K_{eq} = \exp\left(-\frac{\Delta H_r^\circ}{RT} + \frac{\Delta S_r^\circ}{R}\right) = \exp\left(-\frac{3265}{T} + 1.271\right), \quad (2.23)$$

where $K_{eq} = k_{1-2}/k_{2-1}$ [24].

2.4.2 Estimating the Rate Coefficients for the Reverse Reaction

Sirjean et al. only calculated the forward rate coefficients [24]. In order to simulate the thermal decomposition of cyclohexane, rate coefficients for both the forward and the reverse reactions, k_f and k_r , are needed. When the forward rate coefficient k_f and the change in Gibbs free energy $\Delta G^\circ(T)$ are known, the reverse rate coefficient is estimated by using this thermodynamic identity:

$$\Delta G^\circ(T) = -RT \ln(K_{eq}), \quad (2.24)$$

where $K_{eq} = k_f/k_r$. This yields

$$k_r = k_f \exp\left(\frac{\Delta G^\circ(T)}{RT}\right). \quad (2.25)$$

The temperature dependence of Gibbs free energy can be assumed to be linear. This is reasonable as [21]

$$G(T) = H - TS. \quad (2.26)$$

Table 2.2: Rate parameters for the modified Arrhenius' equation at $P=1$ atm and $600 \text{ K} \leq T \leq 2000 \text{ K}$ [24]. k_{1-3} is the rate coefficients for the reaction $1 \rightarrow 3$, where the names of molecules 1 and 3 are listed in Table 2.1.

Rate coefficient	$\log(A)$ s^{-1}	n 1	E_a kcal/mol
k_{1-3}	21.32	-0.972	92.63
k_{3-1}	9.91	0.136	2.09
k_{2-3}	20.11	-0.785	85.77
k_{3-2}	10.38	0.137	2.13
k_{3-4}	2.46	2.569	1.42
k_{3-5}	-1.33	3.800	17.22
k_{3-6}	5.23	2.185	44.25
$k_{3-7/8}$	10.40	0.994	25.75
k_{9-8}	18.53	-0.797	64.85
k_{8-9}	12.21	-0.305	1.98
k_{8-7}	7.32	1.443	3.03
k_{8-10}	5.57	2.171	16.44
$k_{8-11/12}$	2.23	2.995	37.61

2.4.3 Energy Needed to Decompose Cyclohexane

To calculate the energy needed to decompose cyclohexane, the bond dissociation energy is used. A molecule's bond dissociation energy D tells how much enthalpy is required to break a certain bond by homolysis [25]. The bond strength varies a lot with its environment. Table 2.3 illustrates this variation. To find the bond dissociation energy for the molecules in the decomposition of cyclohexane, quantum mechanical calculations may be done for each and every bond of each molecule. Gong et al. did this for some of the molecules; see Figure 2.13. As this process is time consuming, it is rather preferred to use the average bond energy U_b , which is the average of all the bond dissociation energies of a molecule. The relevant average bond energies are listed in Table 2.4.

To calculate the energy needed in the arbitrary reaction



the energy released when forming the $A - B$ bonds is subtracted from the energy needed to break the $B - B$ bonds;

$$U_{breakbonds} = U_{bB-B} - 2 \cdot U_{bA-B}. \quad (2.28)$$

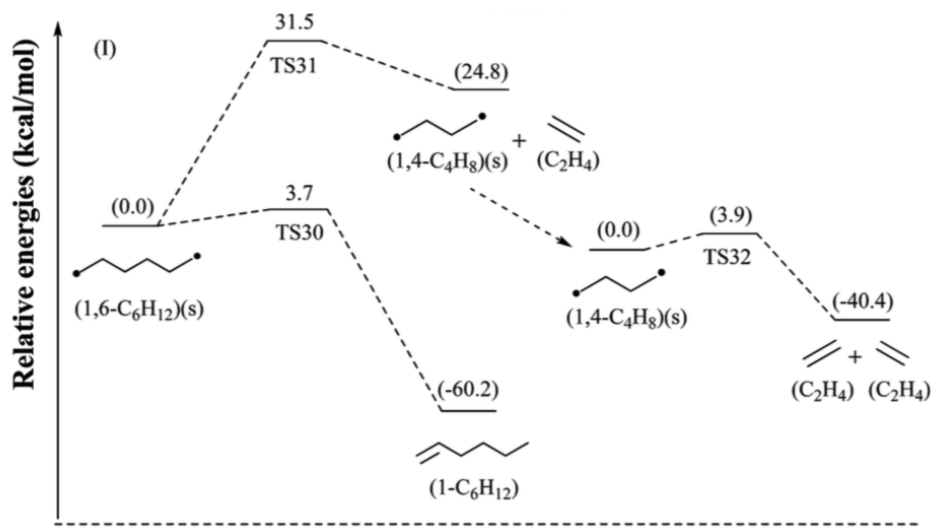
If the net energy is negative, the reaction is exothermic and heat is released from the system to the surroundings.

Table 2.3: Bond dissociation energies D for different bonds of some molecules [26].

Bond	D kJ/mol
$CH_3 - H$	431
$CH_2 - H$	473
$CH - H$	452
$C - H$	337
$CH_3CH_2 - H$	410
$CH_3 - CH_3$	368
$CH_2 = CH_2$	682
$CH_3CH_2CH_2 - H$	410
$(CH_3)_2CH - H$	395

Table 2.4: Average bond energies U_b [27].

Bond	U_b kJ/mol
$H - H$	432
$C - H$	413
$C - C$	347
$C = C$	614

**Figure 2.13:** Potential energy for dissociation of some molecules relative to biradical 1,6-hexane. The energy is in kcal/mol [23].

Method

In the calculations it is assumed that the applied voltage sets up an electric field that is strong enough to partly ionize a thin channel of cyclohexane. The plasma can be caused by impact ionization, photoionization, field ionization or other mechanisms. This is not an important part of the current model and will thus not be considered. To simplify the calculations, it is assumed that the streamer initiation happens in this order:

1. A thin channel is ionized due to the strong electric field from the tip of the electrode.
2. The channel starts to conduct. The electric field changes and available energy is "released".
3. The energy will heat and evaporate the liquid (and gas) in the initiated streamer channel.
4. The pressure in the streamer increases due to the phase change (and the decomposition of the liquid.)
5. The streamer expands adiabatically. It is assumed that the temperature stays constant during the expansion.
6. If the temperature is high enough, the gas in the streamer decomposes. At the same time the excess energy will ionize a new channel in front of the current one.
7. The initiated channel turns conducting. This step is the same as step 2.

Note that this is just an outline of what is happening when a streamer is initiated. In reality some of these reactions do not happen in defined steps, but rather at the same time. A new streamer may also initiate before the previous streamer channel has expanded. In the calculations, step 7 will not be considered. Nor will the ionization of a "new channel" in step 6. However the energy needed to ionize the first initial streamer will be considered.

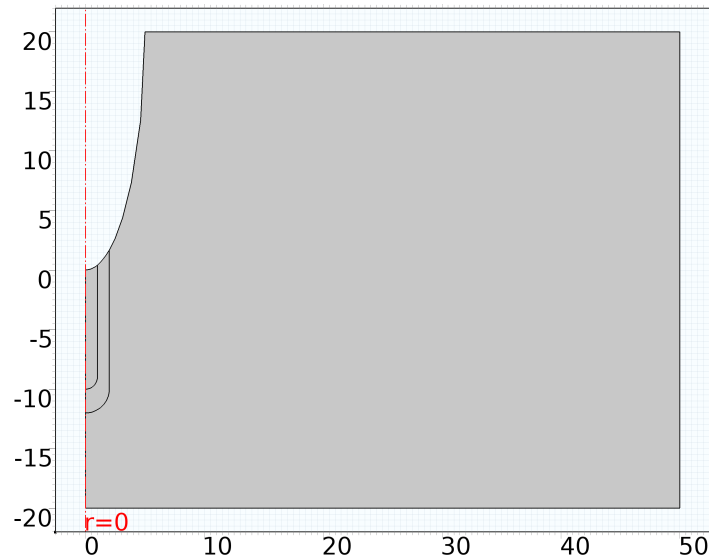


Figure 3.1: The geometry of the electrode tip is modeled as a rotational hyperboloid. The electrode gap $d = 20 \mu\text{m}$. The geometry of the streamer channel is a cylinder with a hemisphere. The units of the axes are in μm .

3.1 Calculating the Available Energy

Before streamer initiation, the energy stored in the electric field can be calculated analytically by using equation (2.2) and (2.5). When the initiated streamer starts to conduct, the electric field changes. As the electric field after the initiation of a channel is rather complex, the potential energy stored in the electric field was calculated numerically, by my supervisor Øystein Hestad, by using the finite element analysis software Comsol. In the Comsol model, the electrode needle is modeled as a rotational hyperboloid. The needle is $20 \mu\text{m}$ long, the tip radius is approximately $2 \mu\text{m}$ and the needle-plane gap is $20 \mu\text{m}$. The model is illustrated in Figure 3.1. In this calculation there are no difference between positive and negative streamers as the model is very simplified.

3.2 Kinetic Monte Carlo Simulation

To predict what products cyclohexane most likely decomposes to, Kinetic Monte Carlo (KMC) simulations are performed. Based on the rate coefficients for the decomposition of cyclohexane, the KMC simulation can be used to model how a chemical reaction evolves with time. According to Guldberg and Waage's law of

mass action for gases, the (forward) reaction rate for reaction (2.11) is

$$r_f = k_f p_A^a p_B^b, \quad (3.1)$$

where p_A and p_B are subject A and B 's partial pressure. Using the ideal gas law, p_i can be rewritten as

$$p_i = \frac{N_i k_B T}{v_i} = c_i k_B T = c_i \frac{p_{total} v_{total}}{N_{total}} = \frac{c_i p_{total}}{c_{total}} \equiv c_i \alpha, \quad (3.2)$$

where c_i is molecule i 's concentration, c_{total} is the total concentration and p_{total} is the total pressure. This yields

$$r_f = k_f (\alpha c_A)^a (\alpha c_B)^b. \quad (3.3)$$

The probability for each reaction j (per time step) is then given by

$$P_j = \frac{r_j}{\sum r_j}. \quad (3.4)$$

In the denominator we sum the reaction rates for all possible reactions. As the reaction is stochastic and has no memory from passed events, the probability for a reaction is independent of the reaction from previous steps. When a reaction happens, the relevant concentrations are updated and the process goes on until the preset time in the simulation expires. As the process follows a Poisson distribution, each time step is of the form

$$\Delta t = \frac{-\log(Rand)}{\sum r_j}, \quad (3.5)$$

where $Rand$ is a random number with a uniform distribution between 0 and 1 [28]. As fast streamers have a propagation velocity $V_p = 1$ km/s, it is assumed that streamers grow, expand and decompose in a couple of microseconds. Hence the KMC simulation is performed for 1-10 μs .

Results

4.1 Energy Stored in the Electric Field

When the streamer is initiated, it goes from non-conducting to conducting. The electric field changes and goes from what is illustrated in Figure 4.1 to what is illustrated in Figure 4.2. Figure 4.3 shows the energy difference in the electric field when a streamer is initiated. The streamer channel's radius c_r ranges from 0.1 to 1 μm , while the channel's length c_l ranges from 1 to 10 μm . The energy difference is biggest when the initiated channel is as long and wide as possible. An increasing voltage will increase the energy difference.

4.2 Heating the Streamer

4.2.1 Regression of Cyclohexane's Heat Capacity

Sirjean et al. calculated cyclohexane's heat capacity for temperatures up to 1500 K based on vibrational frequencies. To estimate the heat capacity for higher temperatures, the heat capacities in [24] are fitted to equation (2.9). The fitted curve is shown in Figure 4.4. The temperature dependence of the heat capacity is

$$C_p(T) = \exp\left(6.1547 - \frac{451.57}{T}\right). \quad (4.1)$$

4.2.2 Energy Needed to Heat and Evaporate the Streamer

Supposing that all the available energy will heat the streamer, the temperature will distribute as in Figure 4.5. All of the liquid will evaporate and the gas will

V_amp=5000, c_l=1e-5, c_r=1e-6, c=0 Time=100 ns
Surface: Electric field norm (V/m)

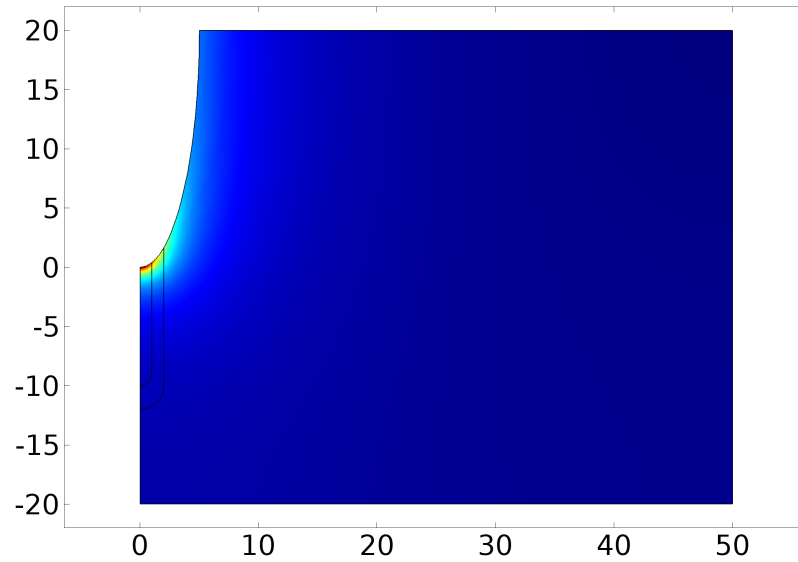


Figure 4.1: The electric field before the channel is conducting. Red indicates a strong field, while blue indicates a weak field. The units of the axes are in μm .

V_amp=5000, c_l=1e-5, c_r=4e-7, c=1 Time=100 ns
Surface: Electric field norm (kV/mm)

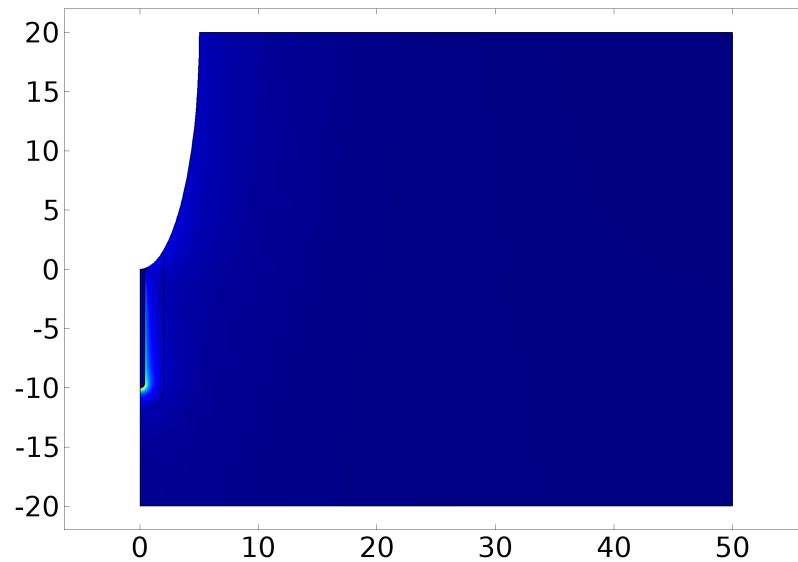


Figure 4.2: The electric field after the channel is conducting. $c_r = 0.4 \mu\text{m}$, $c_l = 10 \mu\text{m}$, $V = 5000 \text{ V}$. Red indicates a strong field, while blue indicates a weak field. The units of the axes are in μm .

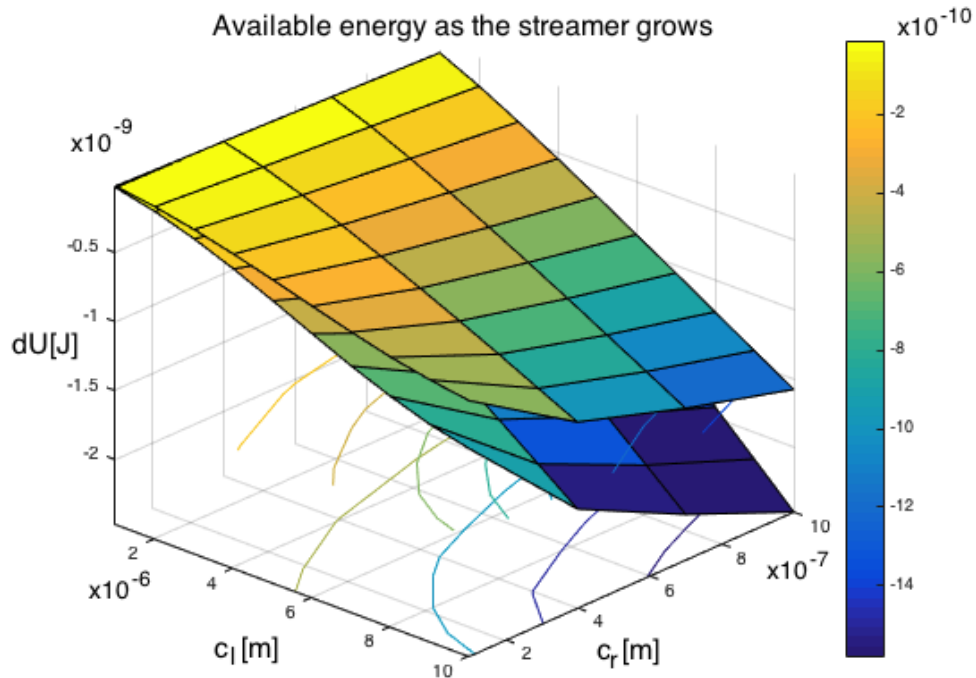


Figure 4.3: Available energy when the streamer goes from non-conducting to conducting for applied voltage $V = 4000$ V (upper surface) and $V = 5000$ V (lower surface).

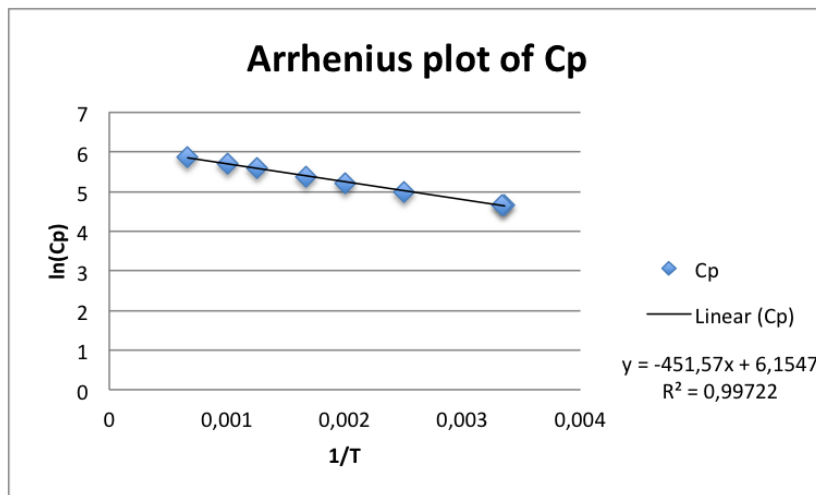


Figure 4.4: Linear regression of the Arrhenius plot of cyclohexane’s heat capacity. The unit of the x-axis is 1/K and the unit of the y-axis is ln(J/(Kmol)).

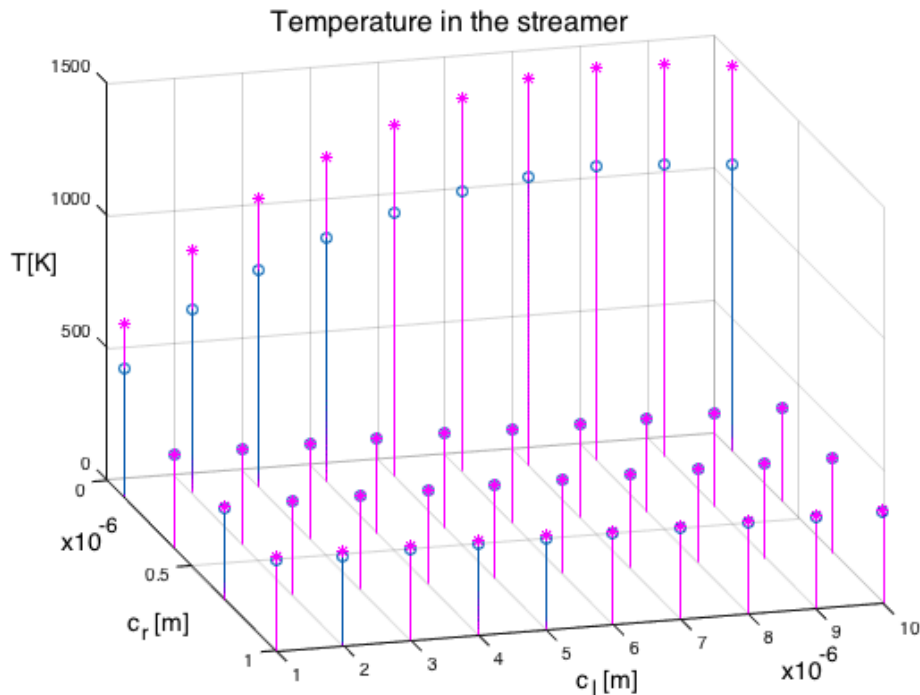


Figure 4.5: The temperature in the streamer if all the available energy is being used to heating and evaporating the liquid. The blue points represent applied voltage $V = 4\text{ kV}$ and the red points represent $V = 5\text{ kV}$.

be heated if the radius of the streamer is $c_r = 0.1\ \mu\text{m}$, but if $c_r \geq 0.4\ \mu\text{m}$ there is barely enough energy to evaporate the liquid. Figure 4.6 shows the temperature in the initiated streamer when the streamer radius is $c_r = 0.1\ \mu\text{m}$. As there is more energy available when the applied voltage is higher, the temperature will be higher for $V = 5\text{ kV}$ than for $V = 4\text{ kV}$. It seems like the available energy reaches a maximum when the length of the streamer is $c_l = 8\ \mu\text{m}$.

4.3 Decomposition of Cyclohexane

4.3.1 Estimating Gibbs Free Energy

Equation (2.25) is used to calculate the reverse rate coefficients for the decomposition of cyclohexane. As this equation depends on Gibbs free energy, the time dependence of ΔG is estimated by doing a linear regression of the Gibbs free energies in Figure 2.10 and 2.11. The fitted curves for ΔG for different reactions are shown in Table 4.1 and the reverse rate coefficients are listed in Table 4.2.

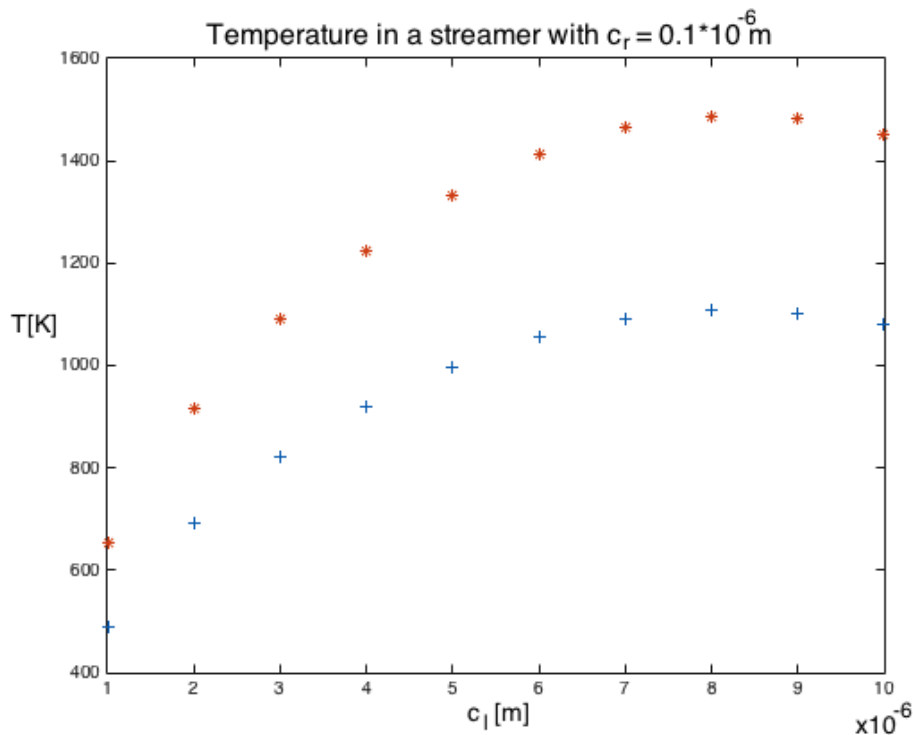


Figure 4.6: The temperature in an initiated streamer with radius $c_r = 0.1 \mu\text{m}$. The blue points represent applied voltage $V = 4\text{kV}$ and the red points represent $V = 5\text{kV}$.

Table 4.1: Linear regression of Gibbs free energy for different reactions.

Reaction	$\Delta G(T)$
Biradical 1,6-hexane \rightarrow 1-hexene	$18.476 T - 290018$
Biradical 1,6-hexane \rightarrow propylcyclopropane	$31.589 T - 261709$
Biradical 1,6-hexane \rightarrow biradical 1,4-butane + ethylene	$-139.47 T + 97627$
Biradical 1,6-hexane \rightarrow cyclopropane	$-67.945 T - 139581$
Biradical 1,4-butane \rightarrow ethylene	$-107.28 T - 182251$
Biradical 1,4-butane \rightarrow 1-butene	$29.205 T - 288613$
Biradical 1,4-butane \rightarrow 1,3-butadiene + hydrogen	$-91.786 T - 177245$

Table 4.2: Calculated reverse rate coefficients.

Rate coefficient	$k_f \exp(\frac{\Delta G^\circ}{RT})$
k_{4-3}	$k_{3-4} \exp((18.476T - 290018)/RT)$
k_{5-3}	$k_{3-5} \exp((31.589T - 261709)/RT)$
k_{6-3}	$k_{3-6} \exp((-67.945T - 139581)/RT)$
$k_{7/8-3}$	$k_{3-7/8} \exp((-139.47T + 97627)/RT)$
k_{7-8}	$k_{8-7} \exp((-107.28T - 182251)/RT)$
k_{10-8}	$k_{8-10} \exp((29.205T - 288613)/RT)$
$k_{11/12-8}$	$k_{8-11/12} \exp((-91.786T - 177245)/RT)$

4.3.2 The Ring Opening Process

Figures 4.7 and 4.8 show the KMC simulation of the first step of the ring opening of cyclohexane i.e. the reaction between the chair formation and boat formation of cyclohexane and biradical 1,6-hexane. In the simulation, there are 10^4 chair-cyclohexane and 0 boat-cyclohexane and 1,6-biradical hexane. The rate coefficients used in the simulation in Figure 4.7, were all given in [24], while in Figure 4.8 the reverse rate coefficients were estimated using equation (2.25). Comparing the two methods, we see that equilibrium is reached approximately at the same time, but significantly more biradical 1,6-hexane is produced when method A) is used than when method B) is used. In lack of better approximations for the reverse rate coefficient, equation (2.25) will still be used when the reverse rate coefficients are not given.

In a streamer with radius and length $c_r = 0.1 \mu\text{m}$ and $c_l = 8 \mu\text{m}$, there are $1.38 \cdot 10^9$ cyclohexane molecules. It is assumed that all of these are chair-cyclohexane. In Figures 4.9, 4.10 and 4.11 the simulation of thermal decomposition of cyclohexane is done for $T = 2000, 3000$ and 4000 K. In the simulation, all the decomposition products from Figures 2.10 and 2.11 are included in the reaction. At $T = 1500$ K cyclohexane starts to decompose to 1,6-biradical hexane after $t = 10 \mu\text{s}$. For $T = 3000$ K the decomposition to other products starts after $t = 1 \mu\text{s}$. Table 4.3 shows the number of each molecule after the liquid has decomposed for $t = 10 \mu\text{s}$ for $T = 3000$ K.

In Figure 4.12 the initial number of molecules were 10^4 chair-cyclohexanes. The number of molecules is much lower than in the ideal initiated streamer from the Comsol model. The effect of decreasing the number of molecules in the KMC simulation is just that equilibrium is reached much faster than in a simulation with more molecules. Figure 4.12 can be used to predict how the decomposition of cyclohexane will look like for a longer time interval. It looks like the most dominating molecules are ethylene and 1-hexene. Note that the result at equilibrium

4.3 Decomposition of Cyclohexane

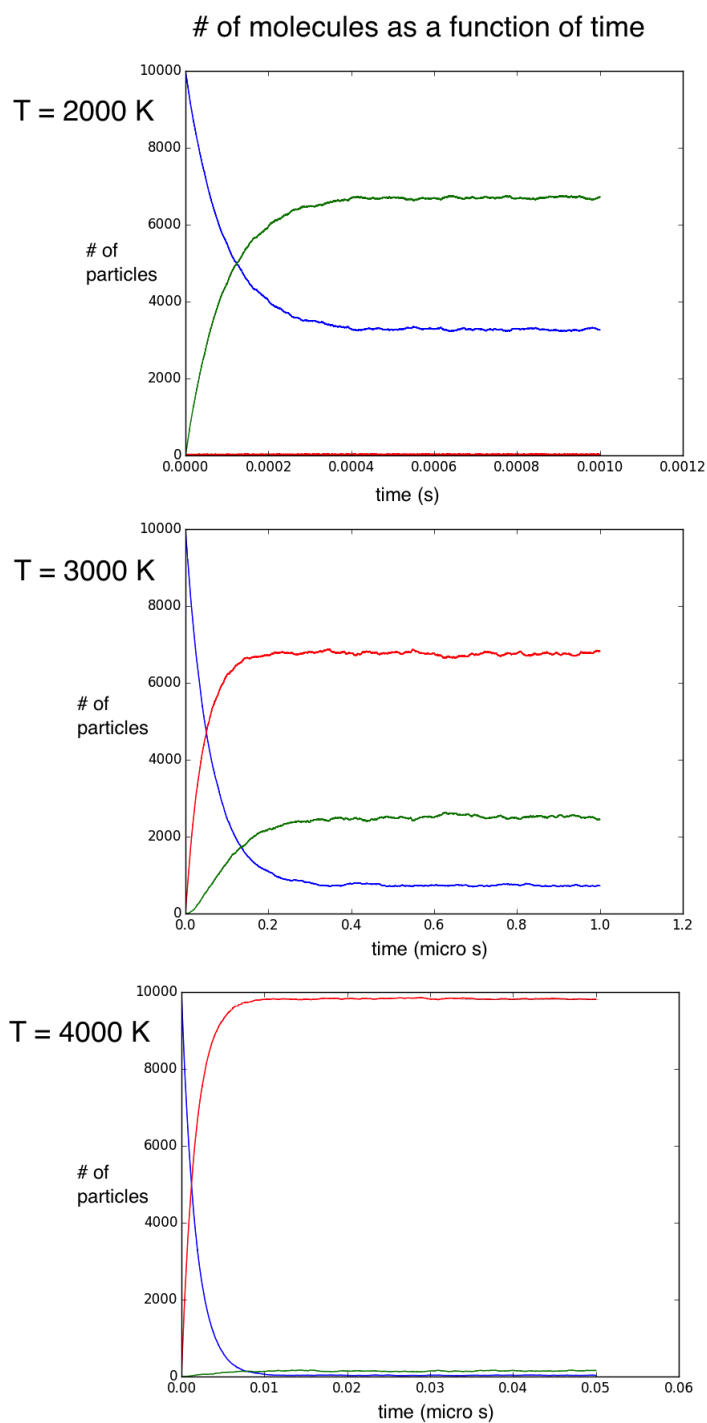


Figure 4.7: Simple ring opening of cyclohexane for $T=2000$, 3000 and 4000 K. All the rate coefficients were given in [24]. Blue is chair-cyclohexane, green is boat-cyclohexane and red is biradical hexane.

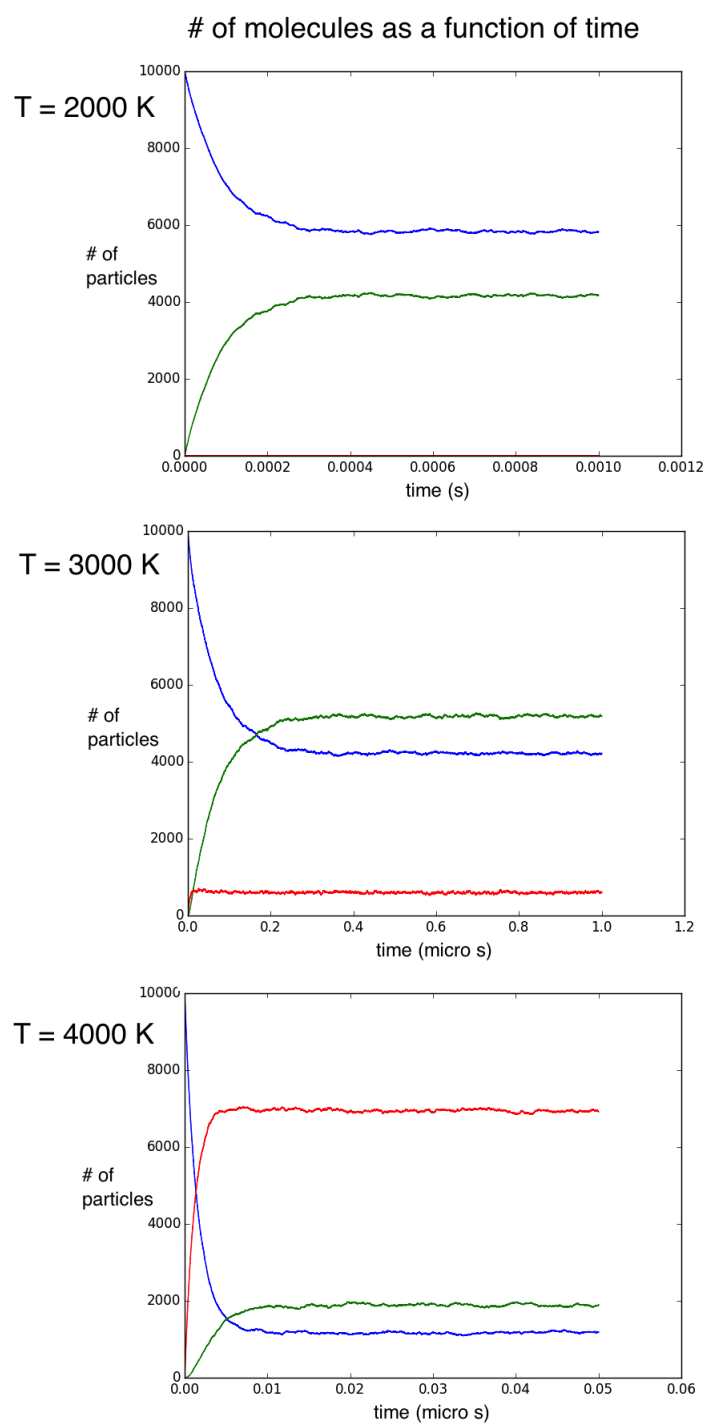


Figure 4.8: Simple ring opening of cyclohexane for $T=2000$, 3000 and 4000 K. All the reverse rate coefficients are estimated. Blue is chair-cyclohexane, green is boat-cyclohexane and red is biradical hexane.

4.3 Decomposition of Cyclohexane

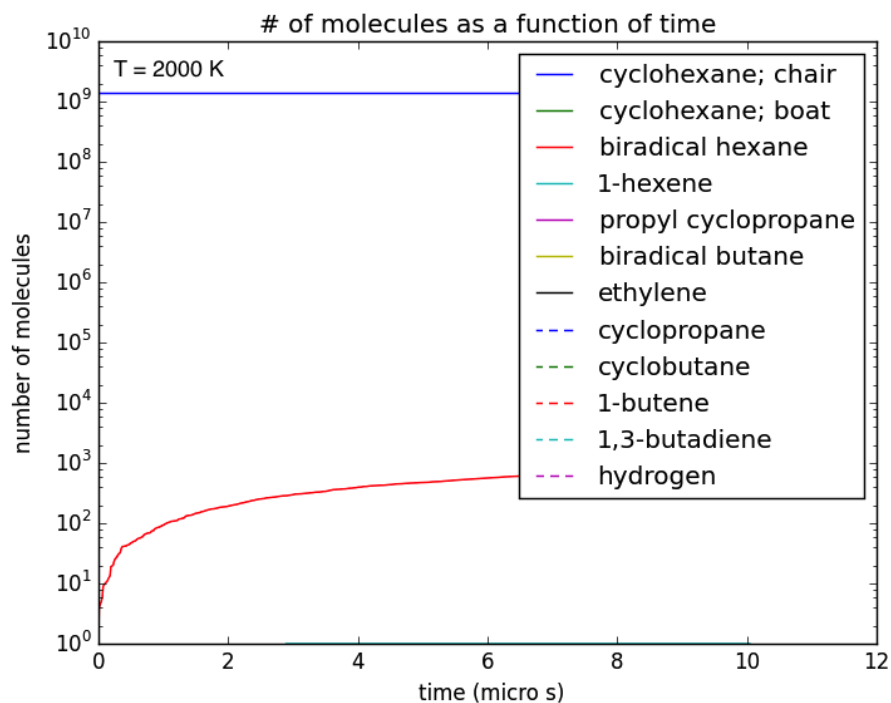


Figure 4.9: Decomposition of cyclohexane at $T = 2000$ K. The fewest possible rate coefficients are estimated.

Table 4.3: The number of molecules at $T = 3000$ K after the simulation had run for $t = 10 \mu\text{s}$.

Molecule	Number of molecules
Cyclohexane (chair)	1 372 794 117
Cyclohexane (boat)	317
Biradical 1,6-hexane	1 547 082
1-hexene	1 109
Propylcyclopropane	255
Cyclopropane	54
Ethylene	5 505
Biradical 1,4-butane	5 442
Cyclobutane	4
1-butene	11
1,3-butadiene	0
Hydrogen	0

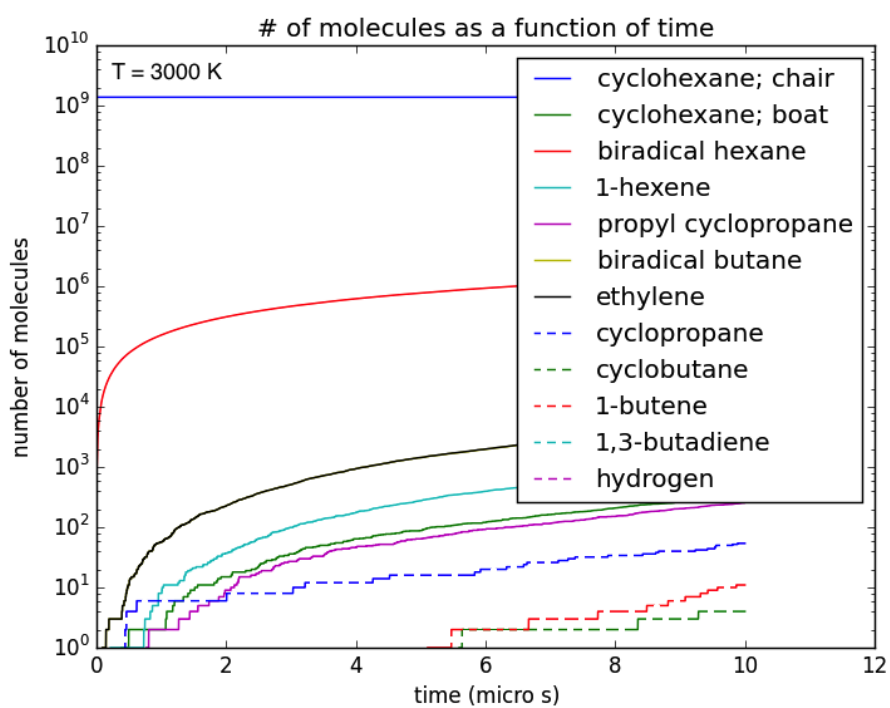


Figure 4.10: Decomposition of cyclohexane at $T = 3000$ K. The fewest possible rate coefficients are estimated.

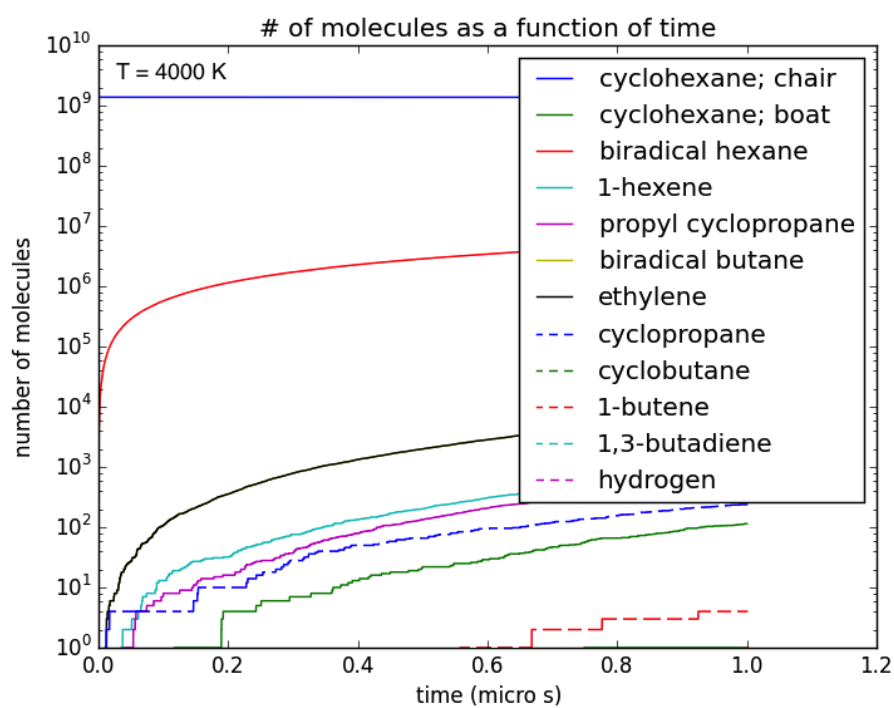


Figure 4.11: Decomposition of cyclohexane at $T = 4000$ K. The fewest possible rate coefficients are estimated.

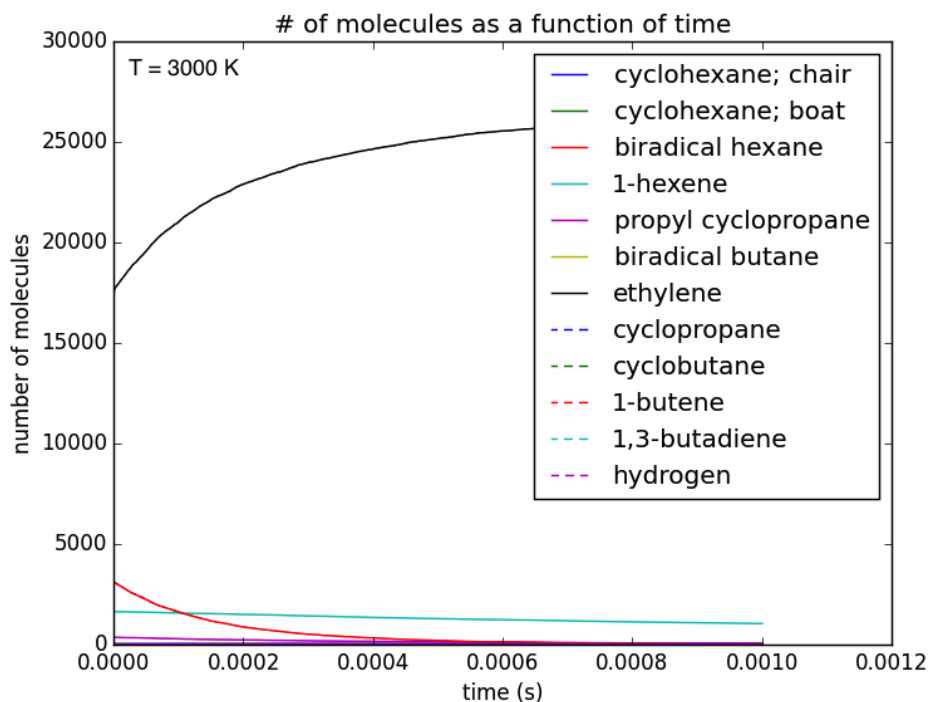


Figure 4.12: Decomposition of 10^4 chair-cyclohexanes at $T=3000\text{K}$.

cannot be used, as the streamer grows before equilibrium is reached.

4.3.3 Energy Needed for Decomposition

In Table 4.4 the energies for each reaction in the decomposition (relative to chair-cyclohexane) $U_{breakbonds}$ are calculated by using equation (2.28). The relative energies calculated by Gong et al. were used whenever possible. Table 4.5 shows the deviation from Gong's data when using the average bond energy to calculate the relative energies. The deviation ranged from 6% to 23%. When the streamer temperature is $T = 3000\text{ K}$, the total energy needed for cyclohexane to decompose to the products in Table 4.3 is $U_{decomposition} = 0.9\text{ pJ}$. For higher temperatures, the KMC simulation lasted too long to get any relevant data.

4.3 Decomposition of Cyclohexane

Table 4.4: Potential energy for the reactions in Figure 2.10 and 2.11 relative to cyclohexane. In the table the reactant is chair-cyclohexane.

Products	$U_{breakbonds}$ kJ/mol
Cyclohexane; boat formation	0
Biradical 1,6-hexane	347
1-hexene	95
Propylcyclopropane	0
2 cyclopropane	0
Ethylene + biradical 1,4butane	451
3 ethylene	282
Ethylene + cyclobutane	104
Ethylene + 1-butene	184
Ethylene + 1,3butadiene + hydrogen	311

Table 4.5: Relative potential energy for the reactions in Figure 2.13 by using quantum mechanical calculations and calculation using bond energy.

Reaction	Energy from [23] kJ/mol	$U_{breakbonds}$ kJ/mol	Deviation
B. 1,6-hexane \rightarrow 1-hexene	-252	-267	6%
B. 1,6-hexane \rightarrow B. 1,4-butane+ethylene	104	80	23%
B. 1,4-butane \rightarrow 2 ethylene	-169	-187	11%

Discussion

5.1 Heating the Streamer

5.1.1 Temperature in the Streamer

According to Figure 4.3 the initiated streamer has more energy the longer and wider it is. Still, all of the liquid in the initiated channel does not evaporate if the initiated streamer radius is $c_r \geq 0.4 \mu\text{m}$. As it is assumed that the streamer is a second mode streamer and that all the liquid in the channel is gaseous, a second mode streamer is initiated only if the channel radius is $c_r = 0.1 \mu\text{m}$. Unsurprisingly, the available energy is higher when the applied voltage is higher. Hence the streamer temperature is higher if the applied voltage is $V = 5000 \text{ V}$ than if it is $V = 4000 \text{ V}$. According to Figure 4.6, the initiated streamer has a maximum temperature $T = 1485 \text{ K}$ when $V = 5000 \text{ V}$ and $c_l = 8 \mu\text{m}$. Ingebrigtsen et al. did a spectral analysis of light emitted from fast streamers in chlorinated hydrocarbon liquids and found that the streamer temperature ranged from 2000 - 7000 K [22]. There is therefore room for improvements in the Comsol model.

In [17] the propagation voltage, when the tip radius was $r_p = 2 \mu\text{m}$ and the gap distance was $d = 2.5 \text{ mm}$, was $V_p = 14 \text{ kV}$. Assuming that the electric field at the electrode tip contributes the most to the available energy and thus determines the initiation voltage, the expected propagation voltage in the Comsol simulation is $V_p = 2.3 \text{ kV}$, according to equation (2.4). To increase the available energy in the calculations and get a higher streamer temperature, the applied voltage in Comsol could of course be increased. However, the applied voltage ranging from 4 to 5 kV should be more than enough to initiate second mode streamers.

To achieve streamers with higher temperature than $T = 1485 \text{ K}$, the simulation should most likely be done with smaller channel radii. Based on Figure 4.5, we know that the whole streamer evaporates if the channel radius is $c_r = 0.1 \mu\text{m}$ and

that it does not evaporate if $c_r \geq 0.4 \mu\text{m}$. To determine the optimal channel radius, it would be interesting to do the same Comsol analysis for $c_r \in [0.01, 0.4]$ with smaller radius steps than in the current model.

5.1.2 The Streamer Radius

According to Figure 4.5, the optimal initiated streamer has $c_r = 0.1 \mu\text{m}$ and $c_l = 8 \mu\text{m}$. By using equation (2.10) and assuming that the streamer only expands radially, the radius of the expanded streamer is $c_{r-exp} = 24 \mu\text{m}$. In [29], shadow-graphic images of the streamers show that the filament radius was 7-15 μm for fast and filamentary streamers. Equation (2.10) also tells that the radius after pressure relaxation would still be $c_{r-exp} = 24 \mu\text{m}$ if the initiated streamer in the Comsol model had a higher temperature. On the other hand, if $c_r = 0.01 \mu\text{m}$ and $c_l = 6 \mu\text{m}$, the radius after relaxation would be $c_{r-exp} = 18 \mu\text{m}$, which is closer to what Ingebrigtsen et al observed for fast streamers [22].

This indicates that increasing the energy (hence increasing the streamer temperature) by applying a higher voltage in Comsol, would not necessarily initiate a second mode streamer, as discussed in the previous subsection. However, a second mode streamer may be initiated if the initial channel radius is smaller than the radius in the current model; $c_r < 0.1 \mu\text{m}$. It should be noted that equation (2.10) assumes that the expanding gas is ideal, which it is not.

5.1.3 Laplacian Field vs. Space Charge Limited Field

The conductivity of dielectrics typically increases exponentially with an increasing electric field. In high field regions, like at the electrode tip, the conductivity is so high that free charges will build up and limit the electric field around the electrode tip. The resulting field is called a space charge limited field (SCLF) [14]. In the Comsol simulation, the electric field is assumed to be Laplacian, meaning that there are no space charges in the surrounding liquid. This is not entirely true as there are some seed electrons in the liquid that will set up a space charge limited field when a high voltage is applied. Figure 5.1 is a comparison of a Laplacian field and a space charge limited field. If assuming SCLF, the available energy when the streamer grows will be higher than with a Laplacian field. This will contribute to a higher energy in the streamer model.

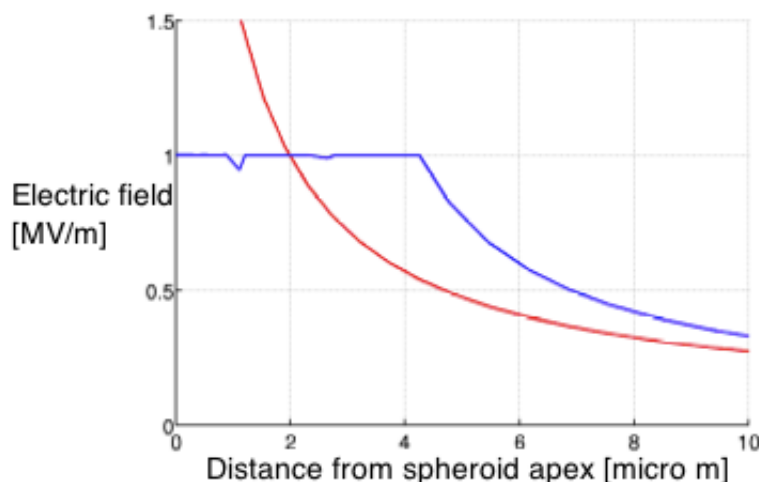


Figure 5.1: The electric field as function of distance from the electrode tip for Laplacian field and SCLF [14]. Red is the Laplacian field and blue is the SCLF.

5.2 Decomposing Cyclohexane

5.2.1 The Decomposition Products

Figure 4.9 indicates that cyclohexane starts to decompose to biradical 1,6-hexane for $T = 2000$ K. This agrees with Felici, who states that there will be decomposition in fast streamers, and with Ingebrigtsen et al., who observed that the temperature in fast streamers can be as low as $T = 2000$ K [10][22]. When $T = 3000$ K the temperature is high enough for cyclohexane to decompose to several other products. The most dominating products are biradical 1,6-hexane, ethylene, biradical 1,4-butane and 1-hexene. The biradicals are unstable products that will decompose even more as time passes. Assuming that the chair formation of cyclohexane keeps decreasing with time, the two dominating products at equilibrium are ethylene and 1-hexene. Figure 4.12, where the simulation ran for a longer time, confirms this. In this simulation the most dominating products are ethylene and 1-hexene, which agrees with what Gong et al. predicted [23].

In Figures 4.7 and 4.8 KMC simulations with estimated and expected rate coefficients are performed. The figures show that the estimated rate coefficients are not the best estimates. Even though equilibrium is reached at the same time as when using the rate coefficients from [24], the number of particles does not agree with expected values. The best solution would be to do quantum mechanical calculations of the reverse reactions, like Sirjean et al. did for the forward rate coefficients in [24]. It should also be noted that the forward rate coefficients in

[24] are for temperatures between 600 and 2000 K. The calculations may therefore be less accurate for higher temperatures.

5.2.2 The Energy Needed to Decompose Cyclohexane

In the Comsol model, the streamer temperature is too low for decomposition of cyclohexane. However, if the temperature had been higher, the liquid had most likely decomposed. In an initiated streamer with $c_r = 0.1 \mu\text{m}$ and $c_l = 8 \mu\text{m}$, the available energy is $U_{available} = 0.8 \text{ nJ}$. After the streamer has been heated up to its boiling point and evaporated, the remaining energy is 0.7 nJ. This is much higher than the energy needed to decompose cyclohexane, $U_{decomposition} = 0.9 \text{ pJ}$. Accordingly the cyclohexane is expected to decompose when the streamer is a second mode streamer or higher, as predicted in [10].

Using average bond energies instead of bond dissociation energies to calculate the change in potential energy, gives estimated energies that deviate a little from the calculated values in [23]. Since the decomposition energy is just a small fraction of the available energy, using the average bond energies instead of the bond dissociation energies will not change the behavior of the streamer drastically. Still, in order to improve the change in the potential energy as cyclohexane decomposes, quantum mechanical calculations can be done like Gong et al. did in [23].

5.3 Ionizing the Gas

In [22] Ingebrigtsen et al. found that the degree of ionization in fast streamers was 1‰. The energy needed to ionize 1‰ of the cyclohexane gas in the initiated streamer (with $c_r = 0.1 \mu\text{m}$ and $c_l = 8 \mu\text{m}$) is $U_{ionization} = 2.2 \text{ pJ}$. As the energy is much lower than $U_{vaporization}$, it is reasonable to assume that there will be some degree of ionization in the initiated streamer. 1‰ ionization is not enough to make the streamer fully conducting, as assumed when a channel is initiated in Comsol. Still, the streamer will be much more conducting than the bulk cyclohexane and therefore it will act as a conductor.

Conclusion

The optimal initial fast streamer has a radius $c_r = 0.1 \mu\text{m}$ and length $c_l = 8 \mu\text{m}$. Assuming that all of the available energy will heat and evaporate the liquid, the temperature in the streamer is $T = 1485 \text{ K}$. Due to the temperature rise, the pressure in the streamer increases and the channel expands in a couple of microseconds. After the channel has expanded, the streamer radius is $c_{r-exp} = 24 \mu\text{m}$. Both the temperature and the expanded streamer radius are out of range compared to what Ingebrigtsen et al. observed for fast streamers. For $T = 1485 \text{ K}$ roughly 1% of the initiated streamer will be ionized, but the liquid will not decompose, as the temperature is too low. However, the energy needed to decompose cyclohexane when $T = 3000 \text{ K}$ is much lower than the energy needed to heat and evaporate the streamer. Hence the decomposition will most likely happen as long as the energy in the streamer is high enough.

For streamers with $c_r = 0.01 \mu\text{m}$ and length $c_l \leq 8 \mu\text{m}$, the streamer radius after pressure relaxation is closer to the observations. If calculations in Comsol were done again, the available energy would be calculated for streamer radii $c_r \leq 0.1 \mu\text{m}$. This comes from a guessing that a smaller radius would result in optimal streamers that are shorter and with higher temperature than in the current model. A higher temperature may also lead to decomposition of cyclohexane, which is predicted for fast streamers.

The estimation of the reverse rate coefficients were not accurate enough, but it is difficult to say how close to reality the estimation is. In the KMC simulation for $T = 3000 \text{ K}$, cyclohexane decomposes to, among other molecules, ethylene and 1-hexene. According to Gong et al. these are the most dominating products in the decomposition of cyclohexane at equilibrium [23]. Still it is difficult to tell if the fraction of each product is realistic or not. To get a better estimation of the rate coefficients, quantum mechanical calculations can be done.

In the Comsol model the electric field is simplified and assumed to be Lapla-

cian. In reality seed electrons and free charges in the dielectric liquid will set up a space charge limited field at the tip of the needle electrode. If assuming a SCLF the potential energy in the electric field at the electrode tip is stronger than if a Laplacian field is assumed. Thus more energy will be available when the streamer is initiated.

In the current model the initiated streamer is as long as half the gap. This is of course not close to what is observed in real experiments. The streamer model is just a simplification used to get a sense of how streamers behave.

Bibliography

- [1] Ildstad E. TET4160 High Voltage Insulation Materials; 2014.
- [2] Atanasova-Hoehlein I. Insulating fluids - Development, trends and influence on diagnostics. In: 3rd International Colloquium Transformer Research and Asset Management; 2014. .
- [3] Devins JC, Rzad SJ, Schwabe R. Breakdown and prebreakdown phenomena in liquids [Journal Article]. *Journal of Applied Physics*. 1981;52(7):4531–4545.
- [4] Lesaint O, Massala G. Positive streamer propagation in large oil gaps - Experimental characterization of propagation modes [Journal Article]. *IEEE Trns Dielectr Electr Insul*. 1998;5(3):360–370.
- [5] Hestad OL, Grav T, Lundgaard LE, Ingebrigtsen S, Unge M, Hjortstam O. Numerical simulation of positive streamer propagation in cyclohexane. In: 2014 IEEE 18th International Conference on Dielectric Liquids (ICDL). IEEE; 2014. p. 1–5.
- [6] Jones HM, Kunhardt EE. DEVELOPMENT OF PULSED DIELECTRIC-BREAKDOWN IN LIQUIDS [Journal Article]. *J Phys D-Appl Phys*. 1995;28(1):178–188.
- [7] Ingebrigtsen S, Smalo H, Astrand PO, Lundgaard L. Effects of Electron-attaching and Electron-releasing Additives on Streamers in Liquid Cyclohexane [Journal Article]. *IEEE Trns Dielectr Electr Insul*. 2009;16(6):1524–1535.
- [8] Ingebrigtsen S. The Influence of Chemical Composition on Streamer Initiation and Propagation in Dielectric Liquids [Theses]. Norwegian University of Science and Technology; 2008.

-
- [9] Ceccato P. Filamentary plasma discharge inside water : initiation and propagation of a plasma in a dense medium [Theses]. Ecole Polytechnique X; 2009.
- [10] Felici NJ. Blazing a fiery trail with the hounds (prebreakdown streamers). IEEE Transactions on Electrical Insulation. 1988;23(4):497–503.
- [11] Massala G, Lesaint O. A comparison of negative and positive streamers in mineral oil at large gaps [Journal Article]. J Phys D-Appl Phys. 2001;34(10):1525–1532.
- [12] Dumitrescu L, Lesaint O, Bonifaci N, Denat A, Notingher P. Study of streamer inception in cyclohexane with a sensitive charge measurement technique under impulse voltage [Journal Article]. Journal of Electrostatics. 2001;53(2):135–146.
- [13] Lewis TJ. A new model for the primary process of electrical breakdown in liquids [Journal Article]. IEEE Transactions on Dielectrics and Electrical Insulation. 1998;5(3):306–315.
- [14] Hestad G. Prebreakdown phenomena in solids and liquids stressed by fast transients: The effect of additives and phase [Theses]. Norwegian University of Science and Technology; 2010.
- [15] Lesaint O, Gournay P. On the gaseous nature of positive filamentary streamers in hydrocarbon liquids. II: Propagation, growth and collapse of gaseous filaments in pentane [Journal Article]. Journal of Physics D: Applied Physics. 1994;27(10):2117–2127.
- [16] Lesaint O, Gournay P. Initiation and propagation thresholds of positive prebreakdown phenomena in hydrocarbon liquids [Journal Article]. Dielectrics and Electrical Insulation, IEEE Transactions on. 1994;1(4):702–708.
- [17] Gournay P, Lesaint O. A STUDY OF THE INCEPTION OF POSITIVE STREAMERS IN CYCLOHEXANE AND PENTANE [Journal Article]. J Phys D-Appl Phys. 1993;26(11):1966–1974.
- [18] Lesaint O, Gournay P. On the gaseous nature of positive filamentary streamers in hydrocarbon liquids. I: Influence of the hydrostatic pressure on the propagation [Journal Article]. Journal of Physics D: Applied Physics. 1994;27(10):2111–2116.
- [19] Moon P, Spencer DE. Field theory handbook: including coordinate systems, differential equations and their solutions. Berlin: Springer; 1961.

-
- [20] Coelho R. Properties of the tip-plane configuration [Journal Article]. *Journal of Physics D: Applied Physics*. 1971;4(9):1266–1280.
- [21] Dill KA, Bromberg S, Stigter D. *Molecular driving forces : statistical thermodynamics in chemistry and biology*. New York: Garland Science; 2003.
- [22] Ingebrigtsen S, Bonifaci N, Denat A, Lesaint O. Spectral analysis of the light emitted from streamers in chlorinated alkane and alkene liquids. *Journal of Physics D: Applied Physics*. 2008 Dec;41(23):235204.
- [23] Gong CM, Li Z, Li X. Theoretical Kinetic Study of Thermal Decomposition of Cyclohexane. *Energy & Fuels*. 2012;26(5):2811–2820.
- [24] Sirjean B, Glaude PA, Ruiz-Lopez MF, Fournet R. Detailed kinetic study of the ring opening of cycloalkanes by CBS-QB3 calculations. *Journal of Physical Chemistry A*. 2006;110(46):12693–12704.
- [25] Gold V, International Union of P, Applied C. *Compendium of chemical terminology : IUPAC recommendations*. 2nd ed. Oxford: Blackwell Scientific Publications; 1997.
- [26] Dean JA. *Lange's Handbook of Chemistry*. 15th ed. New York: McGraw-Hill; 1998.
- [27] Aylward G, Findlay T. *SI Chemical Data*. 5th ed. Milton: John Wiley & Sons Australia; 2002.
- [28] Jansen APJ. *An Introduction to Kinetic Monte Carlo Simulations of Surface Reactions [Electronic Book Section]*. Springer Berlin Heidelberg; 2012.
- [29] Ingebrigtsen S, Lundgaard L, Astrand PO. Effects of additives on prebreakdown phenomena in liquid cyclohexane: II. Streamer propagation [Journal Article]. *J Phys D-Appl Phys*. 2007;40(18):5624–5634.

Appendix **A**

MATLAB code

A.1 `diff_energy.m`

The script use to plot the available energy.

```
function [dU]= diff_energy(V_amp, c_r, c_l, data)
    E_no_ch=data(find(data(:,1)==V_amp & data(:,2)==c_r &
        data(:,3)==c_l & data(:,5)==0),4);
    C_no_ch=2.*E_no_ch./(V_amp(find(data(:,5)==0)));
    E_ch=data(find(data(:,1)==V_amp & data(:,2)==c_r &
        data(:,3)==c_l & data(:,5)==1),4);
    C_ch=2.*E_ch./(V_amp(find(data(:,5)==1)));
    dU=[V_amp(find(data(:,5)==1)),c_r(find(data(:,5)==1)),
        c_l(find(data(:,5)==1)),E_no_ch.*(C_no_ch./C_ch-1)];

    c_lm=unique(c_l);
    c_rm=unique(c_r);
    V_ampm=unique(V_amp);
    for t=1:length(V_ampm);
        E_mat=[];
        for i=1:length(c_lm);
            ind=find(data(find(data(:,5)==1 & data(:,1)==V_ampm(t)),3)==
                c_lm(i))+40*(t-1);
            E_mat=[E_mat,dU(ind,4)];
        end
        surfc(c_lm, c_rm, E_mat);
        title('Available energy when the streamer grows');
        xlabel('c_l [m]');
        ylabel('c_r [m]');
        zlabel('dU [J]');
        hold all
    end
end
```

```
figure(2)
plot(dU(:,4))
```

A.2 plot_energy.m

```
clear all;
load energy_2.mat;
c_lm=unique(c_l);
c_rm=unique(c_r);
E_mat=[];

for i=1:length(c_lm);
    ind=find(c_l==c_lm(i));
    E_mat=[E_mat,E(ind)]
end

hold all
surfc(c_lm, c_rm, E_mat)
```

A.3 Temp.m

The script used to plot the temperature in the initiated streamer.

```
T=dU;

T_0 = 298; %K
T_b = 354; %K
rho = 0.77*10^6; %g/m^3
DelH = 33000; %J/mol
Mm = 84.16; %g/mol

dT = 298:4000;
Cp = exp(6.1547 - 451.57./dT); %Arrhenius plot J/Kmol
cumCp = cumsum(Cp); %J/mol

for i=1:length(dU);
    %Streameren tilnaermes en sylinder med en halvkule
    volume = pi*dU(i,2).^2*(dU(i,3)-dU(i,2)) + 2*pi/3*dU(i,2).^3;
    %Energi som kreves for varme opp til kokepunktet
    T(i,5) = cumCp(354-297)*rho*volume/Mm;
    %Energi som kreves i fordampingen
    T(i,6) = DelH*rho*volume/Mm;
```

```

if (abs(dU(i,4)) - T(i,5)) < 0
    for j = 1:(354-297)
        if cumCp(j)*rho*volume/Mm > abs(dU(i,4))
            T(i,7) = dT(j)-1;
            break
        end
    end
elseif (abs(dU(i,4)) - T(i,5) - T(i,6)) < 0
    T(i,7) = T_b;
else
    T(i,8) = abs(dU(i,4)) - T(i,5) - T(i,6);
    for j = (354-297+1):length(dT)
        if (cumCp(j)*rho*volume/Mm > (abs(dU(i,4)) - T(i,6)))
            T(i,7) = dT(j)-1;
            break
        end
    end
end
end
end

stem3(T(1:40,2),T(1:40,3),T(1:40,7))
hold on
stem3(T(41:80,2),T(41:80,3),T(41:80,7),'*m')
title('Temperature in the streamer');
xlabel('c_r [m]')
ylabel('c_l [m]')
zlabel('T [K]')

```

Appendix B

Python code

B.1 Cyclohexane.py

Kinetic Monte Carlo simulation of decomposition of cyclohexane.

```
from random import random, seed
from math import exp, floor, log, pi
from sys import exit
from array import array
import pylab
import scipy
#import matplotlib.pyplot as plt

#calculating number of cyclohexane molecules in the streamer
radius = 0.1e-6 #meter
length = 8e-6 #meter
mM = 84.16 #molar mass g/mol
N_A = 6.022e23 #Avogadro's constant /mol
rho = 0.7739e6 #cyclohexane's density at T=298K g/m**3

volume = pi*radius**2*(length-radius) + 2/3*pi*radius**3 #m**3
mol = rho*volume/mM #stoffmengde mol
N = rho*volume*N_A/mM #antall molekylar

#simulation of decomposition of cyclohexane
def rates(k, stoich, conc, coeff):
    r = k
    for i in stoich:
        # r = (k[A]*coeff)**a([B]*coeff)**b...
```

```

        r *= (conc[i]*coeff)**(abs(stoich[i]))
        if conc[i] < abs(stoich[i]):
            r = 0.0
            break
    return r

seed(9876543287654)
t = 0.0 #simulering starter i t=0s
t_end = 10e-6 #hvor mange sekunder simuleringen varer i
p_tot = 1.0 #totalt trykk i bar
T = 3000 #temperature in streamer
R = 8.3144621 # Gas constant in J/K mol
#konsentrasjoner av hvert molekyl. Oppdateres for hvert tidssteg
conc = {'chair':N, 'boat':0, 'biradhexane':0, '1-hexene':0,
        'propylcyclopropane':0, 'biradbutane':0, 'ethylene':0,
        'cyclopropane':0, 'cyclobutane':0, '1-butene':0,
        '1,3-butadiene':0, 'hydrogen':0}

k_12 = 1 #hastighetskonstanten fra chair- til boat-formasjon.

#n_init = conc['chair'] + conc['boat'] + conc['biradical'] +
#conc['1-hexene'] #antall molekyler i starten
#p_chair = 1 # = conc['chair']*p_tot/(n_init+n_inert)
#n_inert = (conc['chair']*p_tot)/p_chair-n_init #antall inerte molekyler.

#alle de mulige reaksjonene (fram og tilbake).
#Data fra tabell 9 fra Sirjean et al.(2006).
#Bruker kjente og estimerte reversraterverdier.
reactions = {'R1': {'k':k_12, 'r':{'chair':-1}, 'p':{'boat': 1}},
            'R2': {'k':k_12*(3265/T-1.271), 'p':{'chair': 1},
                  'r':{'boat': -1}},
            'R3': {'k':10**(21.32)*T**(-0.972)*exp(-(4184*92.63)/(R*T)),
                  'r':{'chair':-1}, 'p':{'biradhexane': 1}},
            'R4': {'k':10**(9.91)*T**0.136*exp(-(4184*2.09)/(R*T)),
                  'p':{'chair': 1}, 'r':{'biradhexane':-1}},
            'R5': {'k':10**(20.11)*T**(-0.785)*exp(-(4184*85.77)/(R*T)),
                  'r':{'boat':-1}, 'p':{'biradhexane': 1}},
            'R6': {'k':10**(10.38)*T**(0.137)*exp(-(4184*2.13)/(R*T)),
                  'p':{'boat': 1}, 'r':{'biradhexane': -1}},

            'R7': {'k':10**(2.46)*T**(2.569)*exp(-(4184*1.42)/(R*T)),
                  'r':{'biradhexane':-1}, 'p':{'1-hexene': 1}},
            'R8': {'k':10**(2.46)*T**(2.569)*exp(-(4184*1.42)/(R*T))*
                  exp((18.476*T-290018)/(R*T)),
                  'p':{'biradhexane':1}, 'r':{'1-hexene': -1}},
            'R9': {'k':10**(-1.3)*T**(3.8)*exp(-(4184*17.22)/(R*T)),
                  'r':{'biradhexane': -1}, 'p':{'propylcyclopropane': 1}},
            'R10': {'k':10**(-1.3)*T**(3.8)*exp(-(4184*17.22)/(R*T))*
                  exp((31.589*T - 261709)/(R*T)),

```

```

        'p':{'biradhexane': 1}, 'r':{'propylcyclopropane': -1}},
'R11': {'k':10**(10.4)*T**(0.994)*exp(-(4184*25.75)/(R*T)),
        'r':{'biradhexane': -1}, 'p':{'biradbutane': 1, 'ethylene': 1}},
'R12': {'k':10**(10.4)*T**(0.994)*exp(-(4184*25.75)/(R*T))*
        exp((-139.47*T + 97627)/(R*T)),
        'p':{'biradhexane': 1}, 'r':{'biradbutane': -1, 'ethylene': -1}},
'R13': {'k':10**(5.23)*T**(2.185)*exp(-(4184*44.25)/(R*T)), '
        r':{'biradhexane': -1}, 'p':{'cyclopropane': 2}},
'R14': {'k':10**(5.23)*T**(2.185)*exp(-(4184*44.25)/(R*T))*
        exp((-67.945*T - 139581)/(R*T)),
        'p':{'biradhexane': 1}, 'r':{'cyclopropane': -2}},

'R15': {'k':10**(18.53)*T**(-0.797)*exp(-(4184*64.85)/(R*T)),
        'r':{'cyclobutane':-1}, 'p':{'biradbutane': 1}},
'R16': {'k':10**(12.21)*T**(-0.305)*exp(-(4184*1.98)/(R*T)),
        'p':{'cyclobutane': 1}, 'r':{'biradbutane': -1}},

'R17': {'k':10**(7.32)*T**(1.443)*exp(-(4184*3.03)/(R*T)),
        'r':{'biradbutane':-1}, 'p':{'ethylene': 2}},
'R18': {'k':10**(7.32)*T**(1.443)*exp(-(4184*3.03)/(R*T))*
        exp((-107.28*T-182251)/(R*T)),
        'p':{'biradbutane':1}, 'r':{'ethylene': -2}},
'R19': {'k':10**(5.57)*T**(2.171)*exp(-(4184*16.44)/(R*T)),
        'r':{'biradbutane':-1}, 'p':{'1-butene': 1}},
'R20': {'k':10**(5.57)*T**(2.171)*exp(-(4184*16.44)/(R*T))*
        exp((29.205*T-288613)/(R*T)),
        'p':{'biradbutane':1}, 'r':{'1-butene': -1}},
'R21': {'k':10**(2.23)*T**(2.995)*exp(-(4184*37.61)/(R*T)),
        'r':{'biradbutane':-1}, 'p':{'1,3-butadiene': 1, 'hydrogen': 1}},
'R22': {'k':10**(2.23)*T**(2.995)*exp(-(4184*37.61)/(R*T))*
        exp((-91.786*T-177245)/(R*T)),
        'p':{'biradbutane':1}, 'r':{'1,3-butadiene': -1, 'hydrogen': -1}}
}

```

```

#arrays med floats
plot_t = array('d')
plot_conc = {'chair': array('d'), 'boat': array('d'), 'biradhexane': array('d'),
            '1-hexene': array('d'), 'propylcyclopropane': array('d'),
            'biradbutane': array('d'), 'ethylene': array('d'),
            'cyclopropane': array('d'), 'cyclobutane': array('d'),
            '1-butene': array('d'), '1,3-butadiene': array('d'),
            'hydrogen': array('d')}

```

```

while t < t_end:
    rsum = 0.0
    #Antall molekyler

```

```

n = conc['chair'] + conc['boat'] + conc['biradhexane'] + conc['1-hexene'] +
    conc['propylcyclopropane'] + conc['biradbutane'] +
    conc['ethylene'] + conc['cyclopropane'] + conc['cyclobutane'] +
    conc['1-butene'] + conc['1,3-butadiene'] + conc['hydrogen']
coeff = p_tot/n #Fra ideell gasslov og Guldberg og Waage

for i in reactions:
    r_temp = rates(reactions[i]['k'], reactions[i]['r'], conc, coeff)
    reactions[i]['rate'] = r_temp #legger til midlertidige r i reactions
    rsum += r_temp
rsum_inv = 1.0/rsum
for i in reactions:
    #legger til sannsynligheter (for at en reaksjon skjer) i reactions
    reactions[i]['prob'] = reactions[i]['rate']*rsum_inv

p = random() #tilfeldig tall mellom 0 og 1
p_acc = 0.0 #akkumulert sannsynlighet
for i in reactions:
    p_acc += reactions[i]['prob']
    if p < p_acc:
        #sannsynligheten for at en reaksjon skjer, er proporsjonal med r
        reaction = i
        break

for i in reactions[reaction]['r']:
    #oppdaterer konsentrasjonen av reaktantene til den valgte reaksjonen
    conc[i] += reactions[reaction]['r'][i]
for i in reactions[reaction]['p']:
    #oppdaterer konsentrasjonen av produktene til den valgte reaksjonen
    conc[i] += reactions[reaction]['p'][i]

t += -log(random())*rsum_inv

print t, conc

#legger til oppdaterte tider, konsentrasjoner og entropi i arrayer
# plot_t.append(t)
plot_t.append(t/0.000001)
plot_conc['chair'].append(conc['chair'])
plot_conc['boat'].append(conc['boat'])
plot_conc['biradhexane'].append(conc['biradhexane'])
plot_conc['1-hexene'].append(conc['1-hexene'])
plot_conc['propylcyclopropane'].append(conc['propylcyclopropane'])
plot_conc['biradbutane'].append(conc['biradbutane'])
plot_conc['ethylene'].append(conc['ethylene'])
plot_conc['cyclopropane'].append(conc['cyclopropane'])

```

```

plot_conc['cyclobutane'].append(conc['cyclobutane'])
plot_conc['1-butene'].append(conc['1-butene'])
plot_conc['1,3-butadiene'].append(conc['1,3-butadiene'])
plot_conc['hydrogen'].append(conc['hydrogen'])

#plot the results
pylab.yscale('log')
pylab.plot(plot_t, plot_conc['chair'], label='cyclohexane; chair')
pylab.plot(plot_t, plot_conc['boat'], label='cyclohexane; boat')
pylab.plot(plot_t, plot_conc['biradhexane'], label='biradical hexane')
pylab.plot(plot_t, plot_conc['1-hexene'], label='1-hexene')
pylab.plot(plot_t, plot_conc['propylcyclopropane'], label='propyl cyclopropane')
pylab.plot(plot_t, plot_conc['biradbutane'], label='biradical butane')
pylab.plot(plot_t, plot_conc['ethylene'], label='ethylene')
pylab.plot(plot_t, plot_conc['cyclopropane'], label='cyclopropane')
pylab.plot(plot_t, plot_conc['cyclobutane'], label='cyclobutane')
pylab.plot(plot_t, plot_conc['1-butene'], label='1-butene')
pylab.plot(plot_t, plot_conc['1,3-butadiene'], label='1,3-butadiene')
pylab.plot(plot_t, plot_conc['hydrogen'], label='hydrogen')

pylab.legend(loc='upper right')
pylab.title('# of molecules as a function of time')
pylab.xlabel('time (micro s)')
pylab.ylabel('number of molecules')
#pylab.savefig('test33.png')
pylab.show()

#Regner ut endring i potensiell energi for dekomposisjon
#Energies relative to boat/chair cyclohexane in joule.
#The objects are supposed to be the different reactions,
#but I named them one of the products in each reaction for the simplicity's sake.
energy = {'biradhexane': 347000.0/N_A, '1-hexene': 95000.0/N_A,
          'propylcyclopropane': 0.0/N_A, 'cyclopropane': 0/(2*N_A),
          'biradbutane': 451000.0/N_A, 'cyclobutane': 104000.0/N_A,
          '1-butene': 184000.0/N_A, '1,3-butadiene': 743000.0/N_A,
          'ethylene': 282000.0/(2*N_A)}
totalEnergy=0.0
for molecule in energy:
    if molecule != 'ethylene':
        print molecule, conc[molecule], energy[molecule]
        totalEnergy += conc[molecule]*energy[molecule]
totalEnergy += (conc['ethylene']-conc['biradbutane']-
               conc['cyclobutane']-conc['1-butene']-
               conc['1,3-butadiene'])*energy['ethylene']
print totalEnergy

```
